| OF |

AD
A045131

END
DATE
FILMED
11 -77
DDC

NAVAL POSTGRADUATE SCHOOL
Monterey, California

⑨ Master's **THESIS**

⑥ INVESTIGATION OF HEAT TRANSFER IN
STRAIGHT AND CURVED RECTANGULAR DUCTS
USING LIQUID CRYSTALS THERMOGRAPHY.

by

⑩ Mario do Carmo Durao

⑪ June 1977

Thesis Advisor: ⑫ 77 p.   M. Kelleher

251 450

REPORT DOCUMENTATION PAGE		READ INSTRUCTIONS BEFORE COMPLETING FORM
1. REPORT NUMBER	2. GOVT ACCESSION NO.	3. RECIPIENT'S CATALOG NUMBER
4. TITLE (and Subtitle) Investigation of Heat Transfer in Straight and Curved Rectangular Ducts using Liquid Crystals Thermography		5. TYPE OF REPORT & PERIOD COVERED Engineer's Thesis; June 1977
		6. PERFORMING ORG. REPORT NUMBER
7. AUTHOR(s) Mario do Carmo Durao		8. CONTRACT OR GRANT NUMBER(s)
9. PERFORMING ORGANIZATION NAME AND ADDRESS Naval Postgraduate School Monterey, California 93940		10. PROGRAM ELEMENT, PROJECT, TASK AREA & WORK UNIT NUMBERS
11. CONTROLLING OFFICE NAME AND ADDRESS Naval Postgraduate School Monterey, California 93940		12. REPORT DATE June 1977
		13. NUMBER OF PAGES 77
14. MONITORING AGENCY NAME & ADDRESS(If different from Controlling Office)		15. SECURITY CLASS. (of this report) Unclassified
		15a. DECLASSIFICATION/DOWNGRADING SCHEDULE

16. DISTRIBUTION STATEMENT (of this Report)

Approved for public release; distribution unlimited.

17. DISTRIBUTION STATEMENT (of the abstract entered in Block 20, if different from Report)

18. SUPPLEMENTARY NOTES

19. KEY WORDS (Continue on reverse side if necessary and identify by block number)

Taylor-Goertler vortices
Heat Transfer
Rectangular Curved Channel
Rectangular Straight Channel

Temsheet
Liquid Crystals

20. ABSTRACT (Continue on reverse side if necessary and identify by block number)

A rectangular cross section channel with both straight and curved test sections was used to investigate the effect of Taylor-Goertler vortices on the heat transfer from the curved section by comparing the results with those obtained in the straight section. The flow was heated through the Joulean heating of one of the walls which was made of Temsheet. Liquid crystals were applied on the surfaces of both test

(20. ABSTRACT Continued)

sections. Experiments were run for several values of the volumetric flow rate corresponding to Reynolds numbers between 258 and 920. The average Nusselt number was calculated for each experiment and plotted as function of the Reynolds and Dean numbers. Three distinct regions of the average Nusselt number were observed in the curved section when compared with the straight section. The presence of Taylor-Goertler vortices in the curved section was verified from the distribution of the liquid crystal color bands. It was concluded that the overall effect of the vortices whenever they occurred was to improve the heat transfer process from the curved section.

Investigation of Heat Transfer in
Straight and Curved Rectangular Ducts
Using Liquid Crystals Thermography

by

Mario do Carmo Durao
Lieutenant, Portuguese Navy

Submitted in partial fulfillment of the
requirements for the degrees of

MASTER OF SCIENCE IN MECHANICAL ENGINEERING
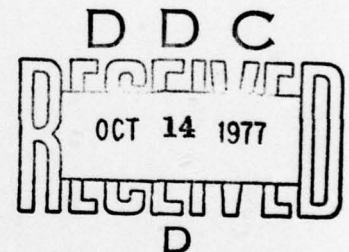
and

MECHANICAL ENGINEER

from the

NAVAL POSTGRADUATE SCHOOL

June 1977

Author _Mário do Carmo Durao_

Approved by: _Matthew Killehn_
                                    Thesis Advisor

Allen E. Fuhs
Chairman, Department of Mechanical Engineering

Robert R. Fossum
Dean of Science and Engineering

ABSTRACT

A rectangular cross section channel with both straight
and curved test sections was used to investigate the effect
of Taylor-Goertler vortices on the heat transfer from the
curved section by comparing the results with those obtained
in the straight section. The flow was heated through the
Joulean heating of one of the walls which was made of
Temsheet. Liquid crystals were applied on the surfaces of
both test sections. Experiments were run for several values
of the volumetric flow rate corresponding to Reynolds num-
bers between 258 and 920. The average Nusselt number was
calculated for each experiment and plotted as function of
the Reynolds and Dean numbers. Three distinct regions of
the average Nusselt number were observed in the curved
section when compared with the straight section. The presence
of Taylor-Goertler vortices in the curved section was veri-
fied from the distribution of the liquid crystal color
bands. It was concluded that the overall effect of the
vortices whenever they occurred was to improve the heat
transfer process from the curved section.

4

TABLE OF CONTENTS

LIST OF TABLES

6

LIST OF FIGURES

7

8

TABLE OF SYMBOLS

Symbol	Meaning	Units
Ac	cross sectional area of the channel	m^2
A_{PL}	area of the wall heater	m^2
Cp	specific heat of air at constant pressure	KJ/Kg °C
d	height of the channel	m
De	Dean number	
Dh	hydraulic diameter	m
Fwo-wi	radiation shape factor	
$\bar{h}$	average heat transfer coefficient	W/m^2 °C
Kair	thermal conductivity of air	W/m °C
K_{INS}	thermal conductivity of insulation	W/m °C
$\dot{m}$	mass flow rate of air	Kg/sec
Nu	local Nusselt number	
$\overline{Nu}$	average Nusselt number	
$\overline{Nu}_c$	average Nusselt number in curved section	
$\overline{Nu}_s$	average Nusselt number in straight section	
Pr	Prandtl number	
p	atmospheric pressure	N/m^2
$\dot{q}$	volumetric flow rate of air	m^3/sec
Qair	heat convected to the air	W
Q_{Li}	heat lost through inner wall	W
Q_{Lo}	heat lost through outer wall	W
Q_P	power supplied	W

Symbol	Meaning	Units
Q_R	heat transferred by radiation	W
Q_{wi}	heat transferred from the inner wall	W
Q_{wo}	heat transferred from the outer wall	W
R	gas constant for air	J/Kg °K
Re	Reynolds number	
Ri	radius of curvature of inner wall	m
R_{PR}	electrical resistance of precision resistor	Ω
R_R	total radiation resistance	m^{-2}
Ta	Taylor number	
T_B	bulk temperature of the flow	°C
T_{EXIT}	flow exit temperature	°C
T_{IN}	flow inlet temperature	°C
T_{INS}	temperature of the insulation	°C
T_{ROOM}	ambient temperature	°C
T_{OUT}	flow outlet temperature after each test section	°C
T_{wi}	average temperature of inner wall	°K
T_{wo}	average temperature of outer wall	°K
U	mean velocity of the flow	m/sec
V_{PR}	voltage across precision resistor	V
V_H	voltage across wall heater	V
$\bar{x}$	dimensionless axial length coordinate	
ε_{wi}	emissivity of inner wall (Plexiglas)	
ε_{wo}	emissivity of outer wall (Temsheet)	
μ	dynamic viscosity of air	Kg/m·sec

Symbol	Meaning	Units
ρ	density of air	Kg/m^3
σ	Stefan - Boltzmann constant	$W/m^2 \, °K$
ΔT	mean temperature difference	°C
ΔT_{INS}	temperature difference in insulation	°C
ΔX_{INS}	thickness of insulation layers	m

ACKNOWLEDGEMENT

The author wishes to express his appreciation to
Professor Matthew Kelleher for his advice and guidance
during the development of this project. Without his
valuable assistance this thesis could not have been
completed. In addition the author wishes to thank Professor
Paul F. Pucci for his comments and advice.

The personnel of the Mechanical Engineering Shop deserve
a special thanks for their assistance in the preparation
of the experimental apparatus.

Finally the author wishes to thank his wife Maria João
for her understanding and encouragement throughout the
course of this study.

I. INTRODUCTION

A. THE TAYLOR-GOERTLER VORTICES

Several studies have shown that a fully developed laminar flow of a viscous fluid along a concave wall does not remain two-dimensional. Instead, the flow forms a system of counter-rotating vortices - the Taylor-Goertler vortices - whose axes are in the direction of the main flow and with secondary velocities in both perpendicular directions as shown in Figure 1. These vortices are caused by the variation in centrifugal forces on the fluid particles at different locations in the flow.

In a curved channel such as used in the present investigation the velocity profile of the fully developed laminar flow is nearly parabolic. The fluid near the center of the channel has a relatively higher velocity and is subjected to greater centrifugal forces than the fluid moving near the walls. Thus, the tendency is for the fluid in the center of the channel to move outward toward the concave wall. The fluid near the concave wall is unable to resist this action and must move in the spanwise direction and then radially inward replacing the central fluid. Once in the center of the channel, this fluid is subjected to the higher flow velocity and the rotation is continued. This cyclic motion forms the counter-rotating Taylor-Goertler vortices.

Figure 1.   Sketch of Taylor-Goertler
Vortices

Although the Taylor-Goertler vortices are laminar vortices, they may affect the transition from laminar to turbulent flow and are therefore important to understanding this phenomenon.

The influence of the Taylor-Goertler vortices may also explain the increase in the observed heat transfer rates from curved walls.

The Taylor-Goertler vortices have similarities to other vortex flows such as the longitudinal vortex rolls developed in the laminar forced convection heating of fluid layers between parallel plates. The striations seen at stagnation points on bluff bodies and the cross hatching observed in reentry vehicles have also been explained, at least in part, by the presence of Taylor-Goertler vortices.

There are many possible applications that could result from investigation and understanding of the Taylor-Goertler vortices. A few of such applications include improved cooling of turbine blades and other external surfaces, reduction of pressure losses in bends and a better understanding of the transition from laminar to turbulent flow. Heat exchangers could be designed to take advantage of the low pressure drop associated with laminar flow and the improved heat transfer characteristics of the flow in the presence of the vortices.

B. BRIEF HISTORY

Lord Rayleigh [Ref. 1] in 1916 was the first to consider the instability of an inviscid fluid rotating symmetrically about an axis. In his study he determined the stability criterion for the inviscid fluid to be that the product of the local circumferential velocity and the local radius of curvature either increases or at least remains constant as the radius increases.

In 1923 G.I. Taylor [Ref. 2] in an extensive analytic and experimental study extended the work of Rayleigh to viscous fluids. In his investigation for the flow between two rotating cylinders, he found that when the inner cylinder rotates and the outer cylinder is stationary the motion of the fluid becomes unstable when the value of the Taylor number defined as:

$$Ta = Re\sqrt{\frac{d}{Ri}}$$

exceeds 41. In the equation above, d is the spacing between the cylinders, assumed small when compared with Ri, the radius of inner cylinder and Re is the Reynolds number based on the circumferential velocity of the inner cylinder and the length d. For values of the Taylor number greater than the critical value a secondary motion sets in and the Taylor vortices occur.

A similar type of instability is observed when a viscous fluid flows in a curved channel due to a pressure gradient acting around the channel. This problem was first considered analytically by W.R. Dean [Ref. 3] for a channel formed by two concentric cylinders where the spacing between the cylinders was small when compared with the radius of the inner cylinder. Dean concluded that the instability will first arise and secondary flow vortices similar to the Taylor vortices will form when the Dean number defined as

$$De = Re\sqrt{\frac{d}{Ri}}$$

is greater than 36. In this case the Reynolds number was based on the mean velocity of the unperturbed flow and the length d.

The analytical work of Dean was later verified by W.H. Reid [Ref. 4] using a simplified method. H. Goertler [Ref. 5] in 1940 studied the stability of laminar boundary layer profiles on slightly curved walls relative to small disturbances. Goertler found that these disturbances were similar to those investigated by G.I. Taylor which led to the instability in the form of vortices. From numerical calculations he concluded that amplified disturbances were produced only on the concave walls. The approximate results obtained by Goertler were verified in 1955 with an exact solution developed by G. Hammerlin as reported by H. Schlichting

[Ref. 6] and more recently by A.M.O. Smith [Ref. 7] through
an extensive numerical analysis.

In 1955, F. Kreith [Ref. 8] investigated the influence
of curvature on heat transfer for fully developed turbulent
flows and reported that the heat transfer from a heated
concave wall was considerably higher than from a convex
wall of the same curvature and under the same conditions
of flow.

L. Persen [Ref. 9] in 1965 was able to relate the increase
in the heat transfer rate from curved walls with the presence
of the Taylor-Goertler vortices. Persen considered the
special cases of a very high and very low Prandtl number and
determined that the overall effect of the vortices was to
increase the rate of heat transfer through the boundary
layer.

In 1970 P. McCormack, et al. [Ref. 10] reported the first
experimental work on the effect of the Taylor-Goertler vor-
tices on the heat transfer. It was pointed out in their
study that in order to explain theoretically the effect of
the vortices, it was necessary to retain the non-linear
terms in the flow equations. This was considered by R.
Kahawita and R. Meroney [Ref. 11] who concluded that the
high-order terms and the normal velocity components of the
main flow become increasingly important at small wave
numbers.

Y. Mori and Y. Uchida [Ref. 12] in 1966, considered
the fully developed forced convective heat transfer between
horizontal flat plates. They observed that when the tem-
perature difference between the plates increased above a
critical value, there was a formation of longitudinal vortex
rolls, similar to the Taylor-Goertler vortices, with the
axes parallel to the flow direction. M. Akiyama, et al.,
[Ref. 13] in 1971 confirmed the onset of these vortices at
a critical Rayleigh number of 1708 for the case of heating
from below.

The published literature concerning the flow and heat
transfer in curved rectangular channels has been rather
limited as reported by R. Shah and A. London [Ref. 14].
In 1970, K. Cheng and M. Akiyama [Ref. 15] developed a
numerical solution for the forced convection heat transfer
in a curved rectangular channel but only for small aspect
ratios (nearly square cross section). Analytic and experi-
mental results for a fully developed constant wall heat
flux square cross section channel were obtained by Y. Mori,
et al. [Ref. 16]. K. Cheng, et al., [Ref. 17] in 1974
solved the Graetz problem in a curved square channel using
a numerical method.

II. INTENT OF THE STUDY

The purpose of this study was to investigate the
effects of the Taylor-Goertler vortices on the heat trans-
fer in a curved rectangular channel and to compare with the
heat transfer in a straight channel of similar cross section.
It was expected that the effect of the vortices would result
from the secondary velocity components transporting heated
fluid from the curved wall toward the center of the channel
and carrying cooler fluid from the center to the curved
wall. It was also expected that the heat transfer process
from the curved wall would show improvement as a consequence
of the presence of the vortices.

For the purpose of this study, a rectangular cross
section channel with both straight and curved test sections
was considered. The results obtained in the curved section
were compared with those obtained in the straight section
to determine the effect of the Taylor-Goertler vortices on
the heat transfer.

An analytical solution for the case of the straight
test section was given by P. McCuen, et al., [Ref. 18] in
their 1962 study. The results obtained in the straight
section were compared with the analytical results of McCuen.

For the curved section, the results obtained in the
present investigation were compared with the numerical

20

solution developed by K. Cheng and M. Akiyama [Ref. 15] for the heat transfer in rectangular curved channels with small aspect ratios.

III. EXPERIMENTAL WORK

A. DESCRIPTION OF THE APPARATUS

A rectangular cross section channel built as described
in Refs. 19 and 20 was modified to include two heated
sections in order to achieve the objective of this study.
The channel was made of two 0.635 cm thick sheets of Plexi-
glas separated by 0.635 cm thick spacers which also formed
the sides of the channel.

The channel was composed of a straight portion 122.0
cm long, a curved section which completed a 180 degrees
turn and a final short straight section as shown in Figure
2. The radius of curvature of the interior concave wall
of the curved portion was 30.5 cm. The cross section of the
channel was 0.635 cm high and 25.4 cm wide with an aspect
ratio of 40 and a cross sectional area of 16.129 square
centimeters. The cross section of the channel at both test
sections is shown in Figure 3.

The working fluid was air which entered the channel
through an aluminum entrance nozzle attached to the
beginning of the straight portion and which was covered
with cheesecloth during the experimental work. At the end
of the channel, the flow was conducted through an aluminum
exhaust nozzle connected by flexible tubing to a Fisher and
Porter Company variable area flow meter, model number
10A3565. This rotometer had a 100% full scale flow rate
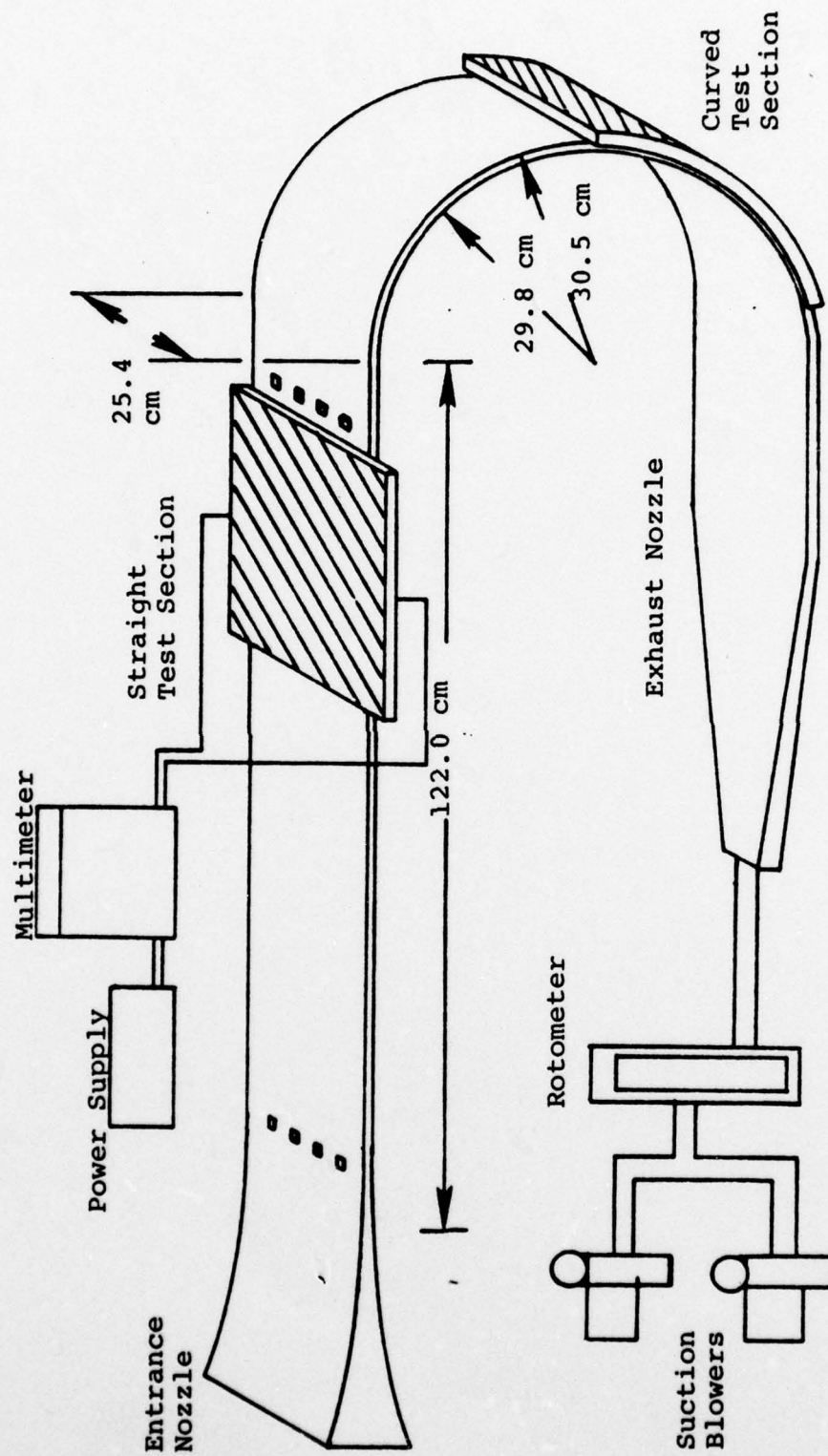
22

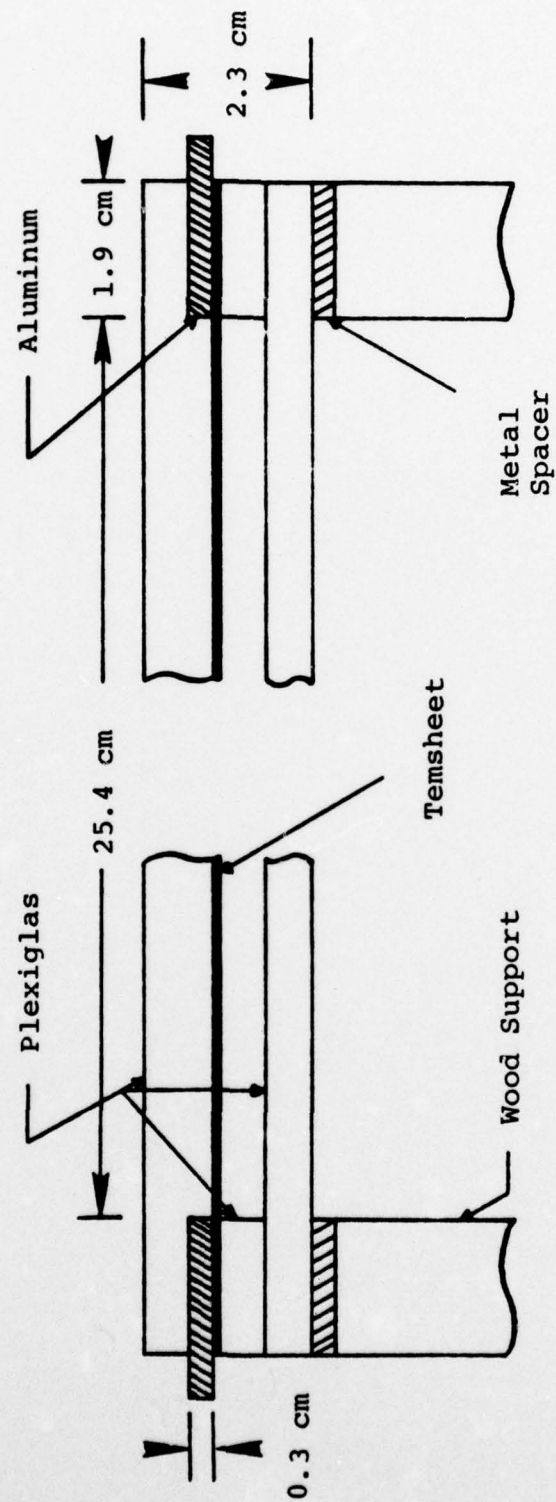Figure 2. Schematic Illustration of Apparatus and Instrumentation

Figure 3. Cross Section of Channel at Both Test Sections

of 0.314 cubic meters of air per minute (11.1 standard cubic feet of air per minute).

The flow of air was drawn through the channel, the flexible tubing and the rotometer by two electrically driven Cadillac centrifugal blowers, model G-12. The blowers were connected in parallel, and their speeds were controlled by varying the motor voltage with a General Radio Company Variac Autotransformer type W10MT3. The voltage was regulated by a Sorenson A.C. voltage regulator, model R1050.

To obtain the experimental heat transfer data, two test sections were constructed: a straight test section 29.2 cm long in the straight portion of the channel after the hydrodynamic entrance region and a curved test section 28.3 cm long subtending an arc of 53.1° in the curved portion of the channel. The area of the straight test section was 741.93 square centimeters and that of the curved test section was 717.74 square centimeters.

In each test section the outer wall was removed and modified as shown in Figures 4 and 5. A piece of Temsheet - a carbon impregnated porous paper with the property of uniform electrical resistivity - was glued to the entire interior surface of the outer wall in each section. The flow of air was heated through the Joulean heating of the Temsheet. As the electrical resistance of the Temsheet was not constant but slowly variable with the temperature, a

Plexiglas

29.2 cm

Thermocouple
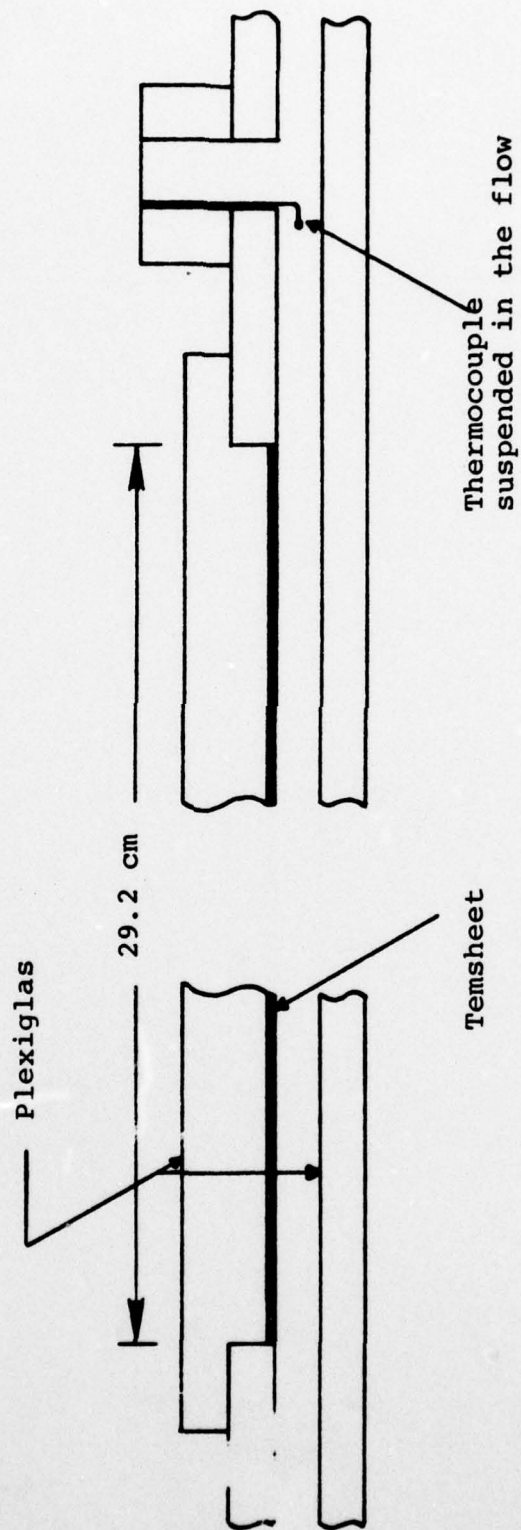suspended in the flow

Temsheet

Figure 4. Internal Arrangement of the Straight Test Section

26

Plexiglas

Temsheet

Thermocouples
on the
Temsheet

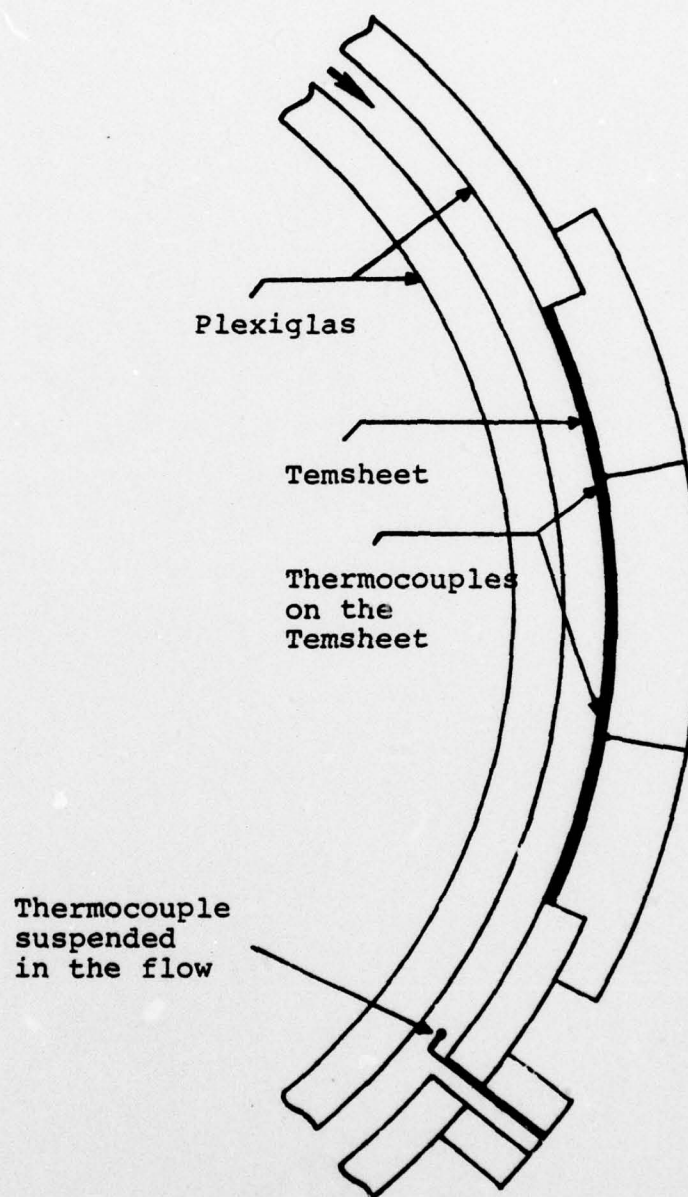Thermocouple
suspended
in the flow

Figure 5. Internal Arrangement of the
Curved Test Section

27

precision resistor with an electrical resistance of 2.013 ohms was inserted into the heating circuit in series with the Temsheet to calculate the instantaneous power supplied. The electrical current to heat the Temsheet was supplied from a LAMBDA Regulated Power Supply model LK345A FM.

The variables to be measured were: the flow inlet temperature at the entrance of the channel (T_{IN}), the flow outlet temperature after each test section (T_{OUT}), the wall temperature of the heated plate in each test section (T_{WO}), the flow exit temperature at the end of the channel (T_{EXIT}), the temperature of the insulation for each test section (T_{INS}) and the voltages across the precision resistor (V_{PR}) and the heater (V_H).

Thermocouples were used to measure the temperatures. Cholesteric liquid crystals were used also to measure qualitatively the surface temperature distribution on the Temsheet. Liquid crystals exhibit dramatic changes in color for small changes in temperature. (An excellent reference on the use of liquid crystals is the article by Cooper, et al. [Ref. 21]). The liquid crystals would provide a reasonable qualitative comparison between the heat transfer process on both test sections through the observation of the distribution of the color bands in each case. The occurrence of color stripes on the curved wall, corresponding to areas of relatively high and low temperature as a result of the presence of the Taylor-Goertler vortices was expected to be observed.

To select the appropriate liquid crystals to be applied on the surface of the Temsheet, the values of the flow inlet temperature, the Reynolds number, the Prandtl number and the Nusselt number were assumed and an approximate energy balance was established:

$$Q = \dot{m} \, Cp \, (T_{OUT} - T_{IN}) = \bar{h} \, A_{PL} \, \Delta T$$

or

$$\frac{\Delta T}{T_{OUT} - T_{IN}} = \frac{Re \; Pr}{Nu} \left(\frac{Ac}{A_{PL}}\right)$$

where

$$\Delta T = Two - \frac{T_{IN} + T_{OUT}}{2}$$

For a desired difference between the outlet and the inlet temperatures of fifteen degrees Celsius, a wall temperature of fifty-five degrees Celsius was calculated.

The required power considering the possible losses was estimated between 45 and 75 watts.

Based on the calculated wall temperature the NCR Micro-encapsulated Liquid Crystal R-53 (onset of red at fifty three degrees Celsius) was selected. After some preliminary experiments, it was found that the response curve of the liquid crystal R-53 allowed for a large variation of the

29

wall temperature within the range of the color blue. It
was then decided to use a combination of three different
liquid crystals instead of a single one in order to obtain
several color bands and a better appreciation of the average
wall temperature. A new Temsheet test section was constructed
and covered with a mixture of the NCR Microencapsulated
Liquid Crystals R-49, R-56 and S-62 prepared in accordance
with Ref. 21 and applied directly to the surface with a
spray gun. About twenty coats were applied to each plate
to obtain a clearly observable differentiation between the
different color bands which it was hoped could be recorded
photographically.

Thirty seven copper-constantan 30 gauge thermocouples
were constructed and inserted at several locations in the
apparatus to measure the different required temperatures.
All the thermocouples were connected to a Honeywell thermo-
couple switch mounted on the side of the apparatus. (See
Figure 6.) In each test section five thermocouples were
inserted between the first and the second layers of the
insulation and another five between the second and third
layers. These thermocouples were connected in parallel
to read an average value of the temperature of the insula-
tion (T_{INS}). Twelve thermocouples, individually connected,
were suspended in the flow, four in the entrance of the
channel, four at the end of the straight test section and
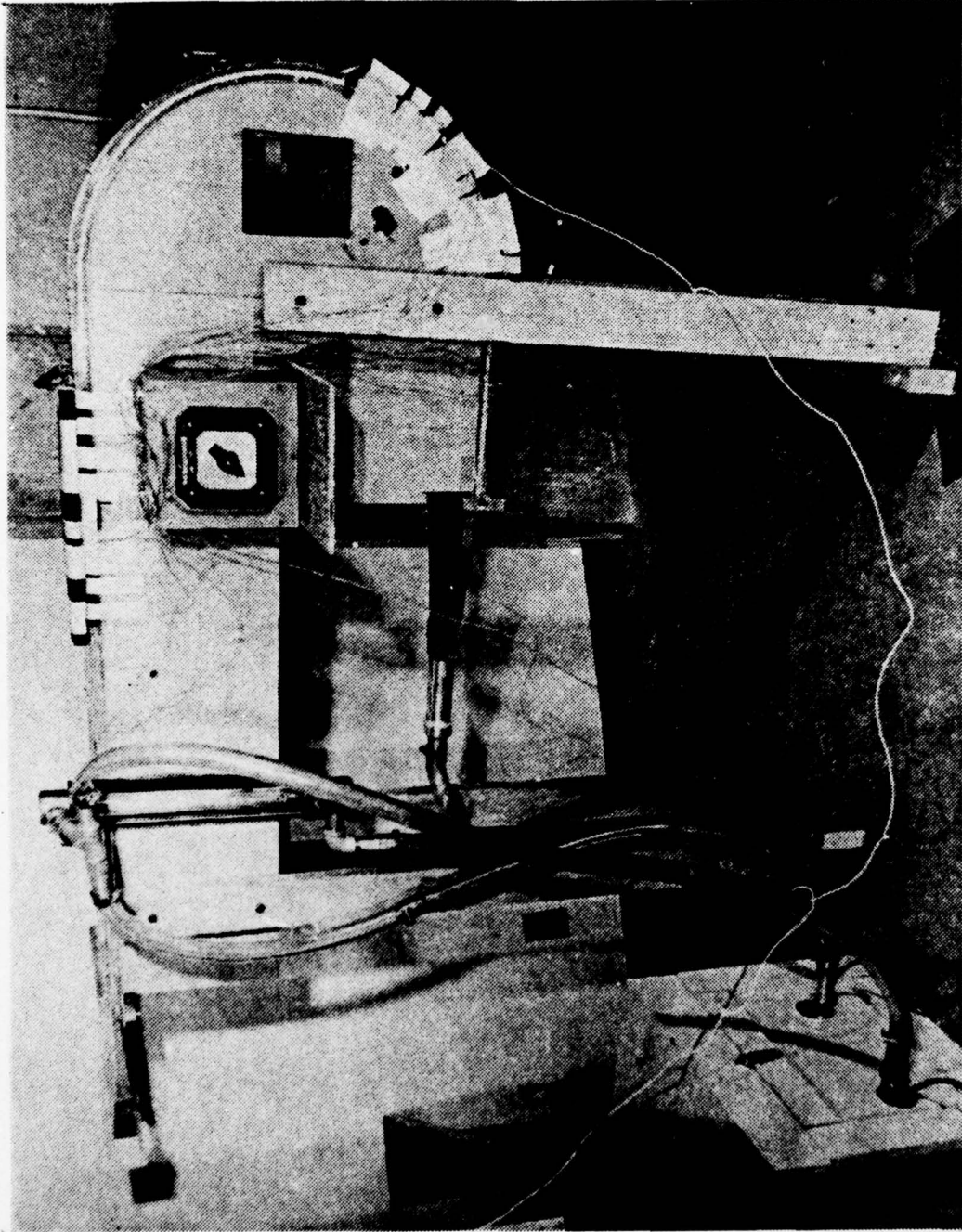the last four at the end of the curved test section. At

30

Figure 6.   The Curved Channel

each one of these locations the thermocouples were distributed spanwise at intervals of 5.0 cm. These thermocouples were used to measure the bulk temperature of the air. In each test section two thermocouples were placed in direct contact with the Temsheet through holes of very small diameter drilled on the middle of each plate at a distance of 10.2 cm from the leading and trailing edges. The beads of these thermocouples were electrically insulated with ENMAR Heat Resisting Glyceryl Phthalate. A final thermocouple was inserted into the flexible tubing close to the rotometer. All the thermocouples were calibrated using a ROSEMOUNT Commutating Bridge, model 920A, and a ROSEMOUNT Calibration Bath, model 913A.

The thermal insulation consisted of ARMSTRONG ARMAFLEX 22 Sheet Insulation - a flexible foamed plastic material. Three layers of insulation, each one with a thickness of 0.635 cm and covering an area slightly larger than each test section, were used. The insulation was fixed in place with the use of Adhesive Corrosion Resistant tape as shown in Figure 7.

To prevent any leakage of air into the channel, the whole apparatus was sealed with DOW CORNING 781 building sealant.

Two aluminum electrodes 0.318 cm thick were inserted between the Temsheet and the plexiglas in each test section
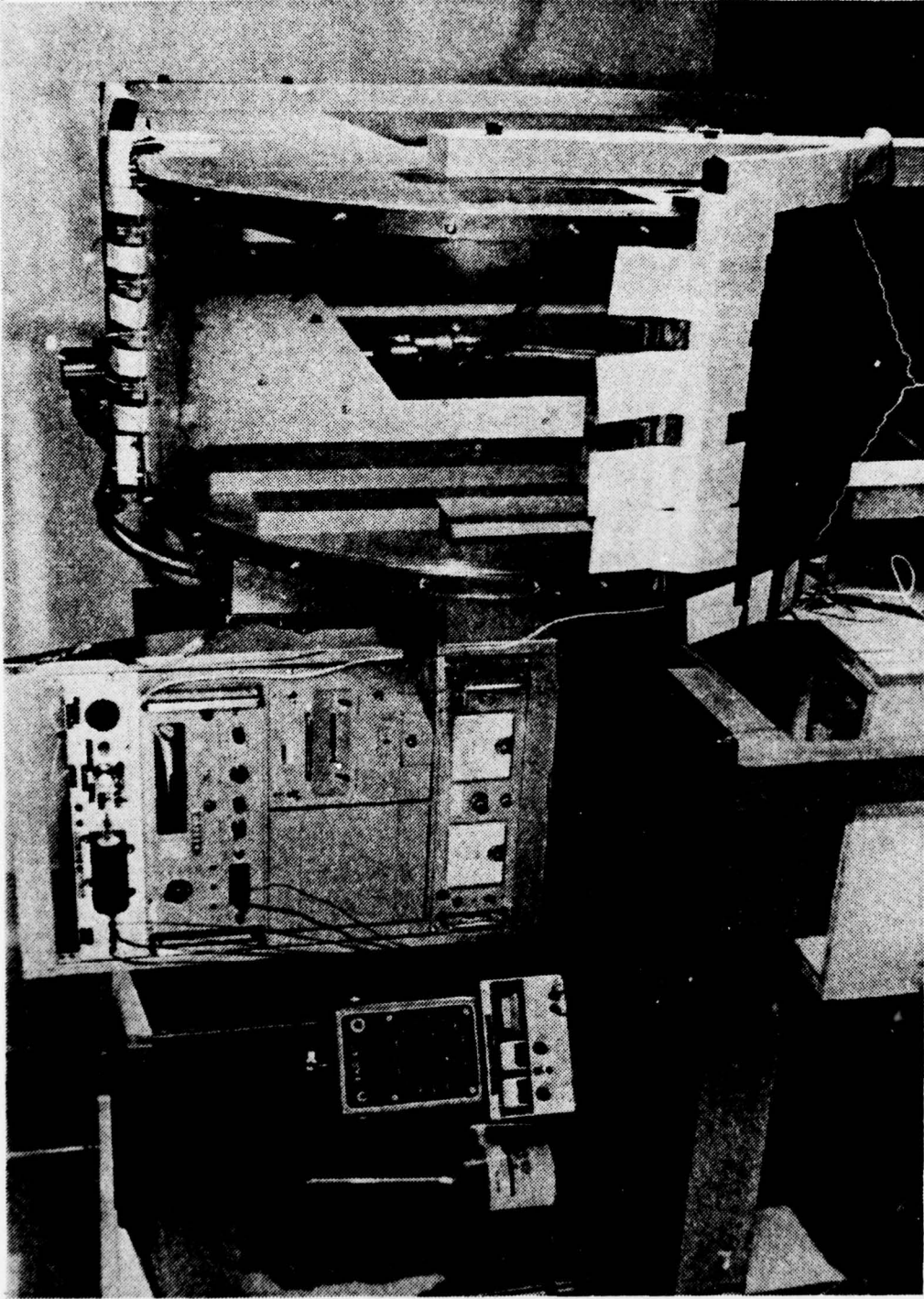
Figure 7. General Arrangement of Apparatus and Instrumentation

as shown in Figure 3. The plates with the Temsheet, the liquid crystals and the aluminum electrodes were assembled in the channel with plastic screws for the purpose of electrical insulation. The Thermocouple Switch was connected to a DYMEC Integrating Digital Voltemeter model 2401B, and to a reference ice bath. A HEWLETT PACKARD Digital Recorder, model 562A, provided an automatic printed record of the instantaneous data for each position of the thermocouple switch.(See Figure 8.)

The general arrangement of the apparatus and the instrumentation is sketched in Figure 2.

B. EXPERIMENTAL PROCEDURES

Experiments were run in each test section for several values of the volumetric flow rate in the range between 0.063 and 0.220 cubic meters of air per minute.

The appropriate electrical power required for each value of the volumetric flow rate in order to heat the Temsheet up to a temperature at which the liquid crystals would change colors was not known. Several preliminary experiments were performed to determine those values of electrical power and also to obtain an appreciation for the general development of the experiments.

Estimates of the required time to reach steady-state, the necessary data to be taken, the frequency of the readings, the overall time of each experiment and the
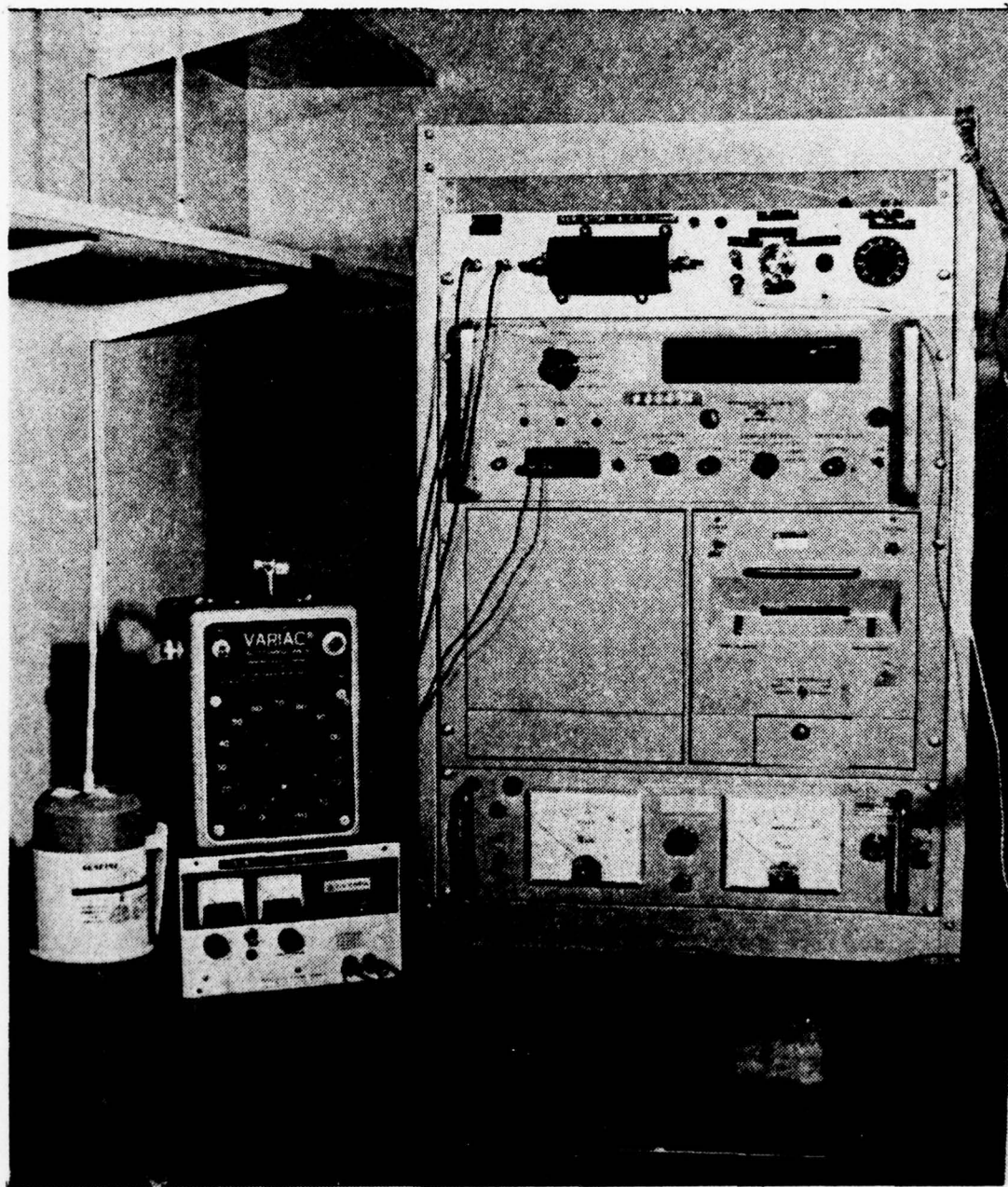
34

Figure 8. Instrumentation

interval between experiments were obtained from the preliminary experiments.

The experiment was considered to have reached steady-state when the variation in the average wall temperature given by the thermocouples in contact with the Temsheet was less than one degree Celsius for a period of ten minutes.

The time to attain steady-state was found to be between one hour and one and one half hours. It was decided that the duration of all experiments would be two hours. Data was taken each half hour during the first hour and every ten minutes in the second hour.

As the area of the curved test section was slightly less than the area of the straight test section, the instantaneous power supplied was different. In order to obtain similar values of dissipated power in both test sections for each value of the volumetric flow rate, the power had to be adjusted for the curved section during the experiment.

The room temperature was determined with a mercury thermometer located in the vicinity of the apparatus. The volumetric flow rate was read directly from the rotometer. The instantaneous values of Tw, T_{EXIT}, T_{INS}, T_{IN} and T_{OUT} were automatically printed by the digital recorder in millivolts. Based on the results of the calibration of the thermocouples, the standard thermocouple tables were used to convert millivolts to degrees Celsius.

The voltages across the precision resistor (V_{PR}) and the heater (V_H) were recorded in volts, and the instantaneous power supplied (Q_p) was then computed using the expression:

$$Q_P = \frac{V_{PR}}{R_{PR}} V_H$$

where R_{PR} was the electrical resistance of the precision resistor, previously determined as 2.013 ohms.

Prior to each experiment, an ice reference bath was prepared and used for the single reference thermocouple connected in series with the thermocouple switch.

The steady-state distribution of the liquid crystal color bands on the surface of both test sections was sketched for most of the experiments and photographed for the case of the curved test section using a Nikomat 35 mm camera with a Nikon 55 mm f 3.5 Macro-Nikkor lens.

During the preliminary experiments the bulk temperature thermocouples produced anomolous readings. Determining the cause required considerable time. An energy balance on the straight test section indicated the value of power transmitted by the heater to the air flow to be greater than the power supplied to the heater.

It was thought at the beginning that leakage of air into the channel could be the cause. However it was later shown that the problem consisted of erroneous temperature readings given by the thermocouples suspended in the flow.

37

These thermocouples had been inserted into the channel through Plexiglas plugs which could be removed for replacement of any defective thermocouple.

Several tests were performed, and it was determined that there was an electrostatic interaction between the Plexiglas plugs and the beads of the thermocouples. The recorded values of the temperature were from two to five degrees Celsius higher than the actual values. This distortion was more evident for the higher values of the volumetric flow rate. The response time of the thermocouples also was much slower than normal. This was confirmed by removing the thermocouples from the apparatus and observing the approach to room temperature. It was found, however, that once the thermocouple beads were removed from the vicinity of the Plexiglas plugs they would read correct values of temperature with a normal response time. As the height of the channel was only 0.635 cm, it was difficult to move the thermocouple beads away from the Plexiglas plugs.

Considering that the problem probably resulted from some electrostatic charge induced in the Plexiglas and transmitted to the beads it was decided to try different materials for the construction of the plugs. Phenolic resin fiberboard and pine wood were used, but the same unsatisfactory results were obtained.

Finally it was decided to devise a process to insert the thermocouples into the channel without the use of the plugs and also to bend the thermocouples in order to place them parallel to the air flow as shown in Figures 4 and 5. When this was accomplished, the correct data was obtained.

IV. PRESENTATION OF DATA

A. ANALYSIS

Since Temsheet has the property of uniform electrical resistivity, the heated wall was considered to be a constant heat flux surface. Also because of the large aspect ratio, the channel was considered to be approximately parallel plates. It was therefore assumed that the experimental configuration represented forced convection between parallel plates with one surface subjected to constant heat flux and with some heat loss at the opposite surface. To analyse this situation several quantities were defined and calculated as follows:

The average heat *transfer coeff*icient between the heated wall and the flow of air in each test section was defined by the equation

$$Qair = \bar{h} \, A_{PL} \, \Delta T$$

In this equation, Qair was the heat convected. (See the Figure in Appendix B.) $\bar{h}$ was the average heat transfer coefficient, A_{PL} was the area of the heated surface and ΔT was the difference between the average wall temperature (Two) and the bulk temperature of the fluid (T_B). The bulk temperature was defined as the arithmetic average of the fluid inlet temperature (T_{IN}) and the fluid outlet temperature (T_{OUT}). In mathematical form ΔT was expressed by:

40

$$\Delta T = Two - T_B = Two - \frac{T_{IN} + T_{OUT}}{2}$$

The heat convected (Qair) was calculated with the equation

$$Qair = \dot{m} \; Cp \; (T_{OUT} - T_{IN})$$

where Cp was the specific heat of air at constant pressure and $\dot{m}$ was the mass flow rate of air given by the product of the volumetric flow rate ($\dot{q}$) and the density of the air (ρ). This density was computed assuming perfect gas behavior at atmospheric pressure and using the flow exit temperature (T_{EXIT}).

The average Nusselt number was then computed from the average heat transfer coefficient through the expression:

$$\overline{Nu} = \frac{\overline{h} \; d}{Kair}$$

where d was the height of the channel and Kair was the thermal conductivity of the air at the bulk temperature (T_B).

The Reynolds number was calculated for all the experiments and defined as:

$$Re = \frac{\rho \; U \; d}{\mu}$$

where

$$U = \frac{\dot{q}}{Ac}$$

Ac was the cross sectional area of the channel and μ was the dynamic viscosity of the air at the flow exit temperature (T_{EXIT}).

For the experiments in the curved test section, the Dean number defined by:

$$De = Re \sqrt{\frac{d}{Ri}}$$

was also calculated. In this equation, d was the height of the channel and Ri was the radius of curvature of the interior surface of the convex wall.

The heat lost by conduction through the outer plate and the insulation was determined with the expression:

$$Q_{LO} = \frac{\Delta T_{INS}}{(\Delta X_{INS}/K_{INS} A_{PL})}$$

where ΔX_{INS} was the thickness of each layer of insulation, K_{INS} was the thermal conductivity of the insulation and ΔT_{INS} was the difference in the temperatures given by the thermocouples located between the first and second layers and those located between the second and third layers.

In order to verify that Qair as measured by the
temperature rise in the air was actually the convection
heat transfer from the Temsheet, an estimate of the radiation
heat transfer in the channel had to be made. To facilitate
this, one experiment was run in which the temperature of
the lower plate was measured with two thermocouples. For
this experiment the radiated heat transfer was computed
with the expression:

$$Q_R = \frac{\sigma (Two^4 - Twi^4)}{R_R}$$

where σ is the Stefan-Boltzmann constant and R_R was the
total resistance to radiation heat transfer between
the plates given by:

$$R_R = \frac{1}{A_{PL}} [\frac{1}{\varepsilon_{wo}} + \frac{1}{\varepsilon_{wi}} - 1]$$

In this expression ε_{wo} is the emissivity of the interior
surface of the outer plate (Temsheet) and ε_{wi} is the
emissivity of the interior surface of the inner plate
(Plexiglas).

A sketch of the control volume for the energy balance
indicating the different components involved and the sample
calculations, for the case in which the radiated heat
transfer was also computed, are given in Appendix B.

43

B. RESULTS

The data collected from the experiments was evaluated
through the expressions described in the previous section
as illustrated in Appendix B, and the results for the major
variables involved are shown in Table I for the straight
test section and in Table II for the curved test section.
A plot of the natural logarithm of the Reynolds number
versus the natural logarithm of the average Nusselt number
is given in Figure 9 for both test sections. The incertainty
bands are shown for two representative points. Sample
calculations for obtaining these incertainty bands are
shown in Appendix A. Figure 10 is a plot of the natural
logarithm of the Dean number versus the natural logarithm
of the average Nusselt number for the curved test section.

The results indicated an increase in the heat transfer
rates with increasing values of Reynolds number for both
test sections. However, when comparing the plotted values
of the average Nusselt number for the curved section with
those of the straight section, three distinct regions were
detected in the curved section. For the highest values
of Reynolds number corresponding to the highest values of
the volumetric flow rate, the Nusselt numbers for the
curved test section were greater than those of the straight
test section. For the lowest values of Reynolds number,
the opposite was noticed with greater heat transfer rates
occurring in the straight test section. A transition region
was observed for intermediate values of Reynolds number.

44

Table I

SUMMARY OF RESULTS FOR STRAIGHT SECTION

Re	Q_p (W)	Qair (W)	ΔT (°C)	$\bar{h}$ (W/m² °C)	$\overline{Nu}$
920	70.35	53.42	34.65	20.77	5.002
782	63.69	47.44	31.69	20.18	4.832
663	61.12	44.13	31.36	18.96	4.562
526	55.74	38.05	29.31	17.50	4.181
401	50.56	33.30	27.98	16.04	3.842
267	47.91	28.04	26.95	14.02	3.321

Table II

Summary of Results for Curved Section

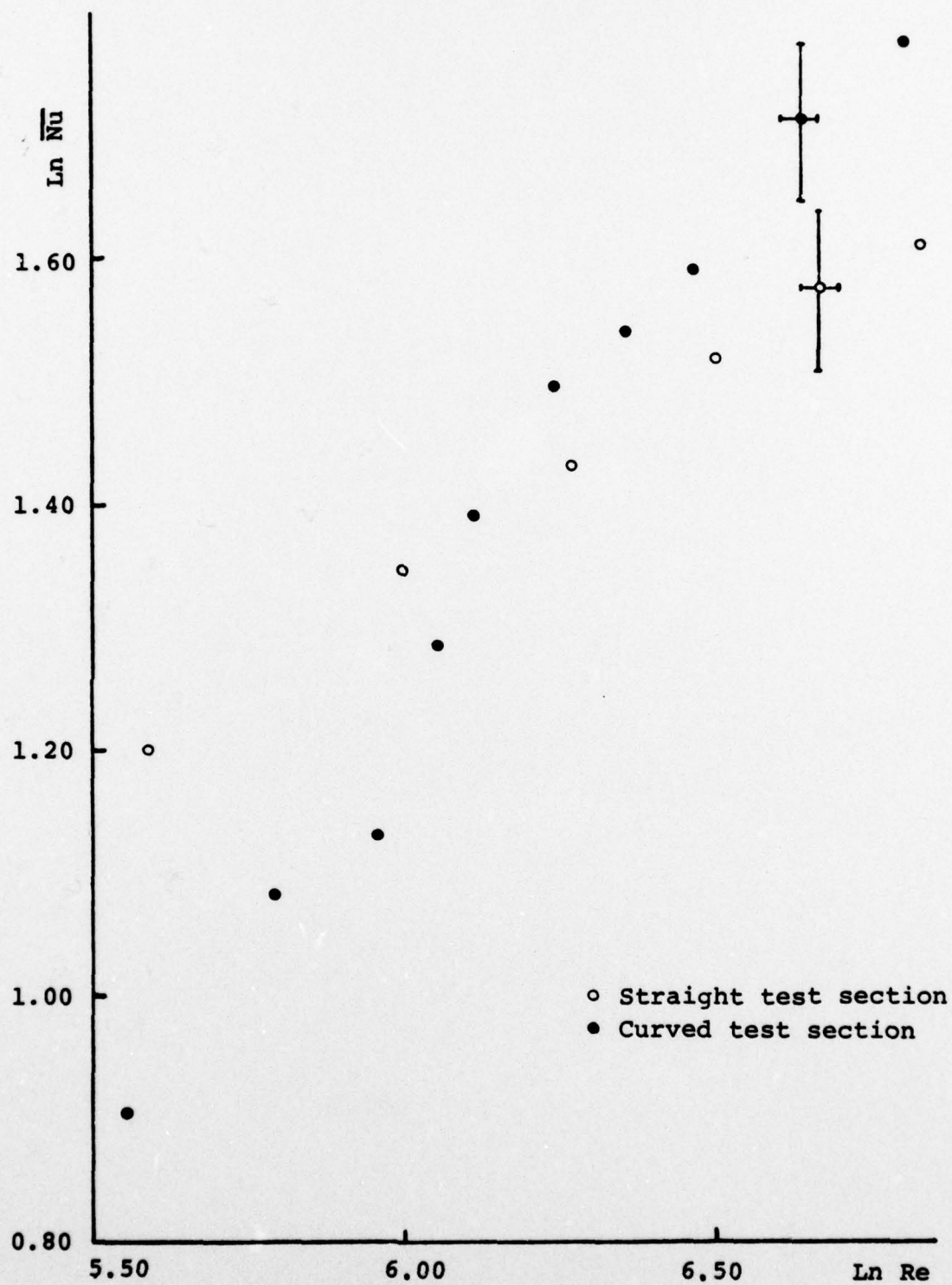| Re	De	Q_P (W)	Qair (W)	ΔT (°C)	$\bar{h}$ (W/m^2 °C)	$\overline{Nu}$
892	130	70.33	54.81	31.09	24.55	5.885
758	111	63.85	47.98	28.77	23.23	5.537
638	93	61.14	43.54	29.68	20.43	4.894
573	84	58.50	40.74	29.19	19.44	4.659
512	75	55.75	36.39	27.34	18.69	4.467
450	66	53.07	35.43	29.39	16.79	4.016
425	62	52.01	33.48	30.84	15.12	3.614
386	56	50.57	30.24	32.50	12.96	3.095
327	48	49.14	28.78	29.39	12.23	2.956
258	38	47.89	24.81	32.78	10.54	2.478

46

Figure 9. Natural Logarithm of Reynolds Number
versus Natural Logarithm of Average
Nusselt Number for Both Test Sections
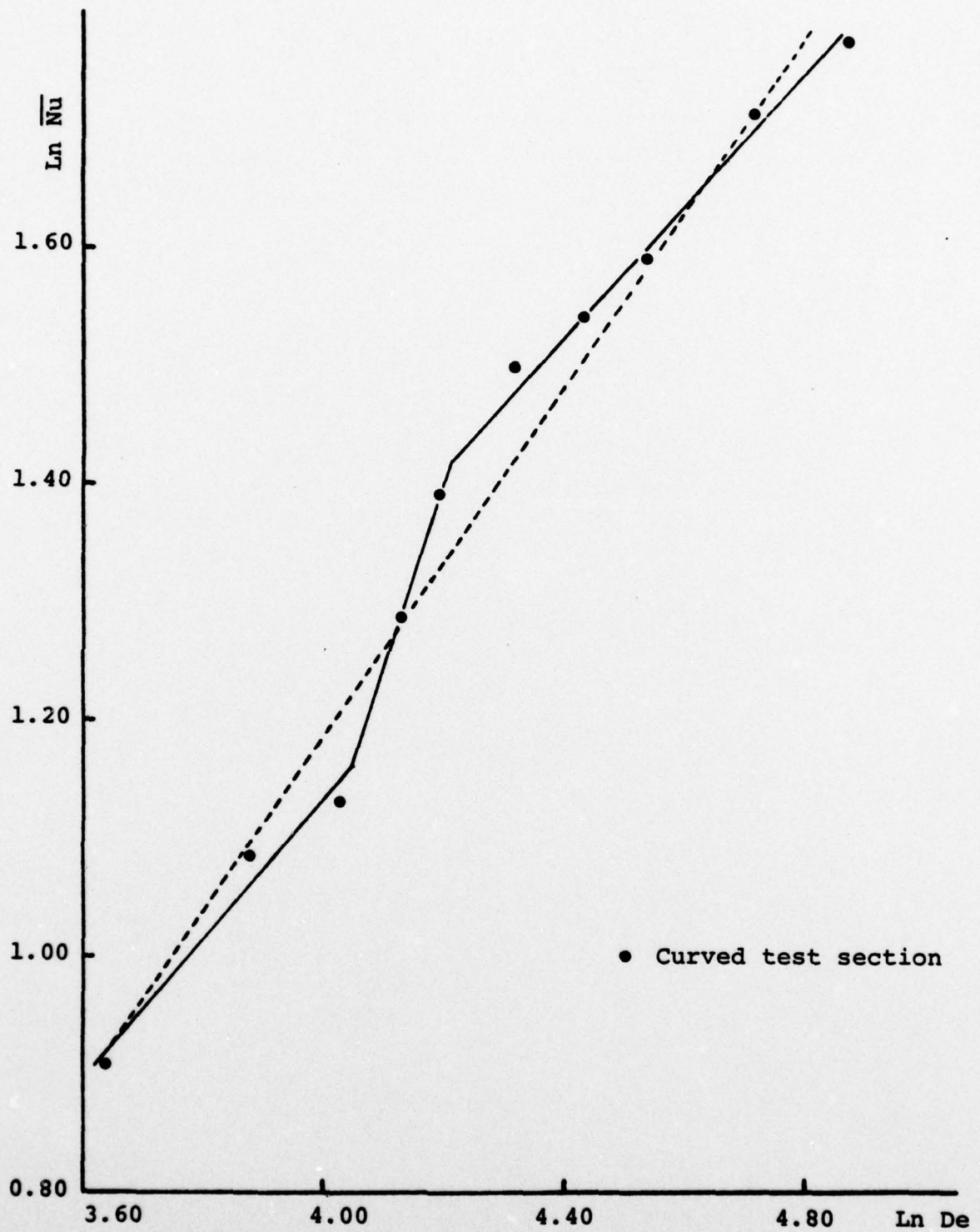
Figure 10.   Natural Logarithm of Dean Number versus
             Natural Logarithm of Average Nusselt
             Number for Curved Test Section

48

These differences in heat transfer behavior for the
curved section as compared with the straight section were
then related to the occurrence of Taylor-Goertler vortices
through the observation of the distribution of the liquid
crystal color bands on the surface of the curved section
for the different values of Reynolds number. It was observed
that for the smallest values of Reynolds number the differ-
ent color bands occurred in almost straight lines perpendicu-
lar to the direction of the flow. The same had been verified
in the straight section independently of the value of Reynolds
number. It was then observed that as the Reynolds number
was increased for the curved section, color stripes oriented
in the streamwise direction, became visible in the region
close to the trailing edge. These color stripes were ex-
plained by the presence of the Taylor-Goertler vortices
and, for the highest values of the Reynolds number, could
be seen over the entire surface of the curved test section.
Schematic drawings of the distribution of the color bands
on the surface of the straight and curved test sections are
shown in Figures 11, 12, 13 and 14.

The occurrence of color stripes and consequently Taylor-
Goertler vortices at the same values of the Reynolds number
for which the average Nusselt numbers were greater in the
curved test section led to the conclusion that the effect
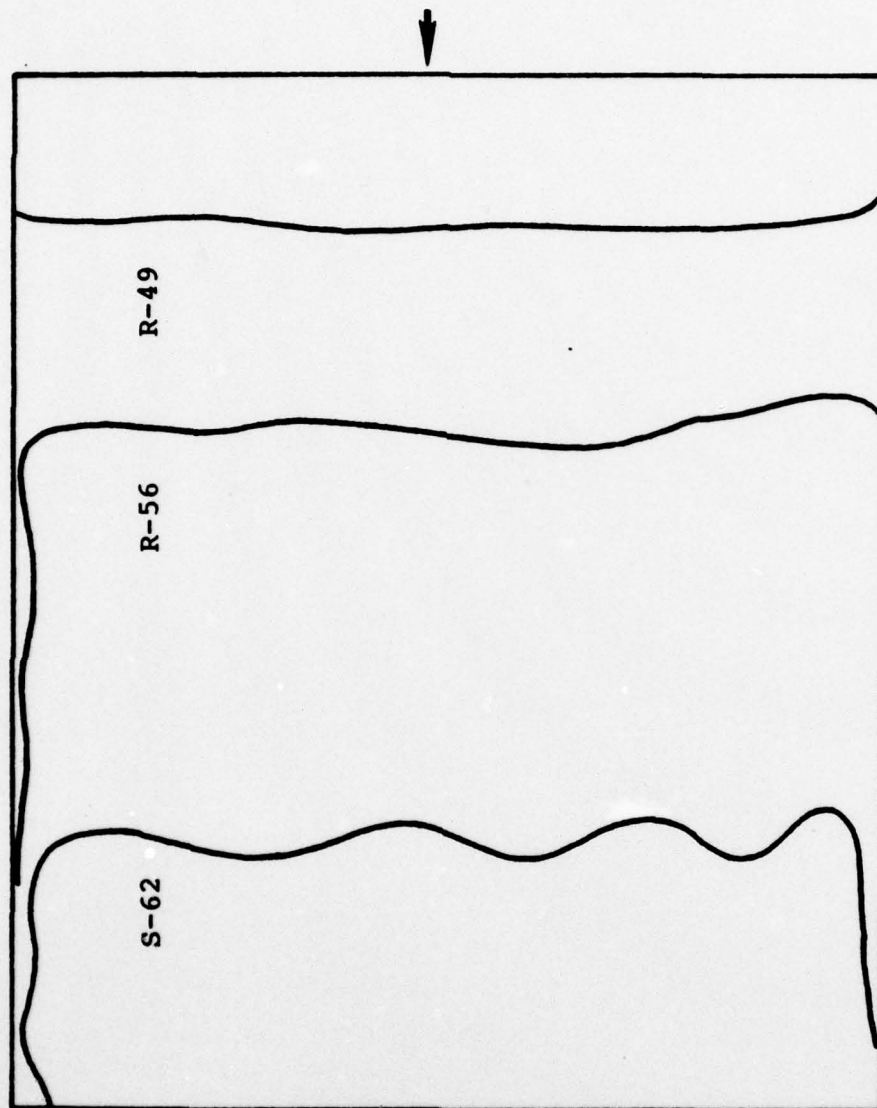of the vortices was to increase the heat transfer rates
from the curved section.

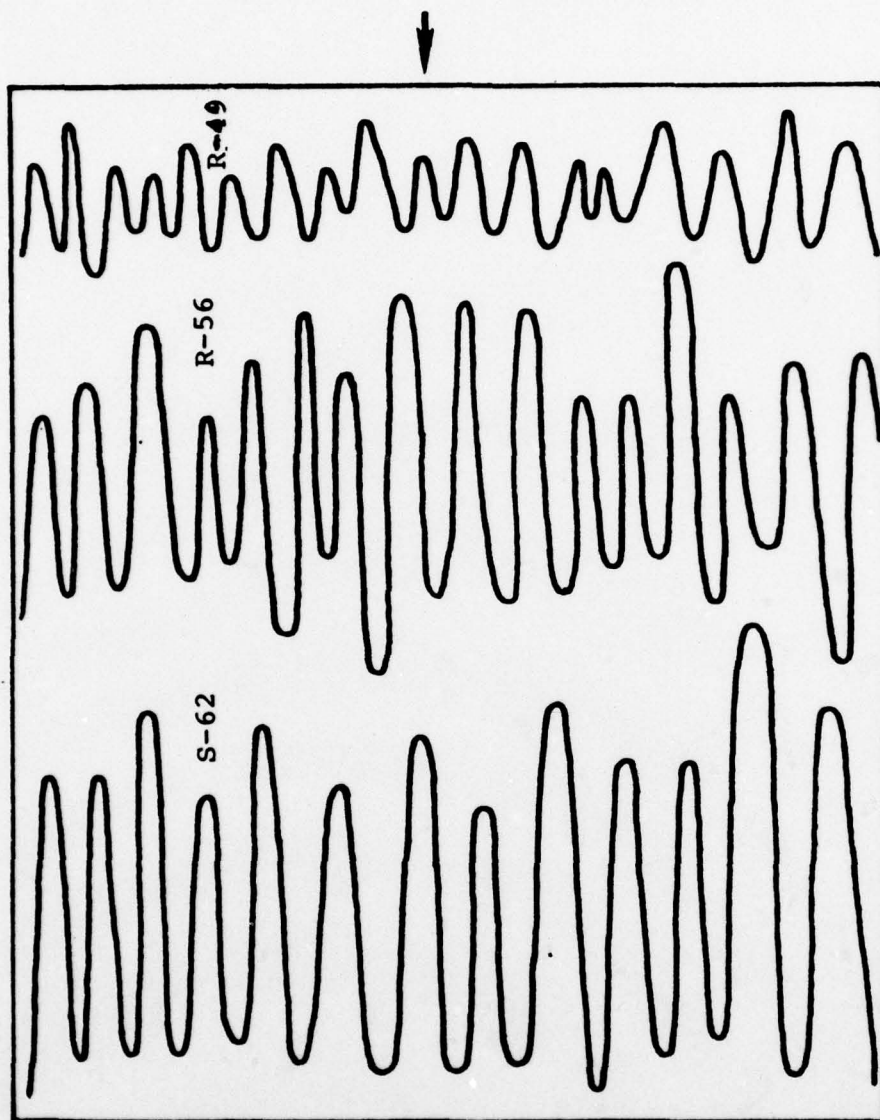Figure 11. Distribution of Liquid Crystal Color Bands in Straight Test Section for Re = 526

Figure 12. Distribution of Liquid Crystal Color Bands in Curved Test Section for Re = 638 (De = 93)

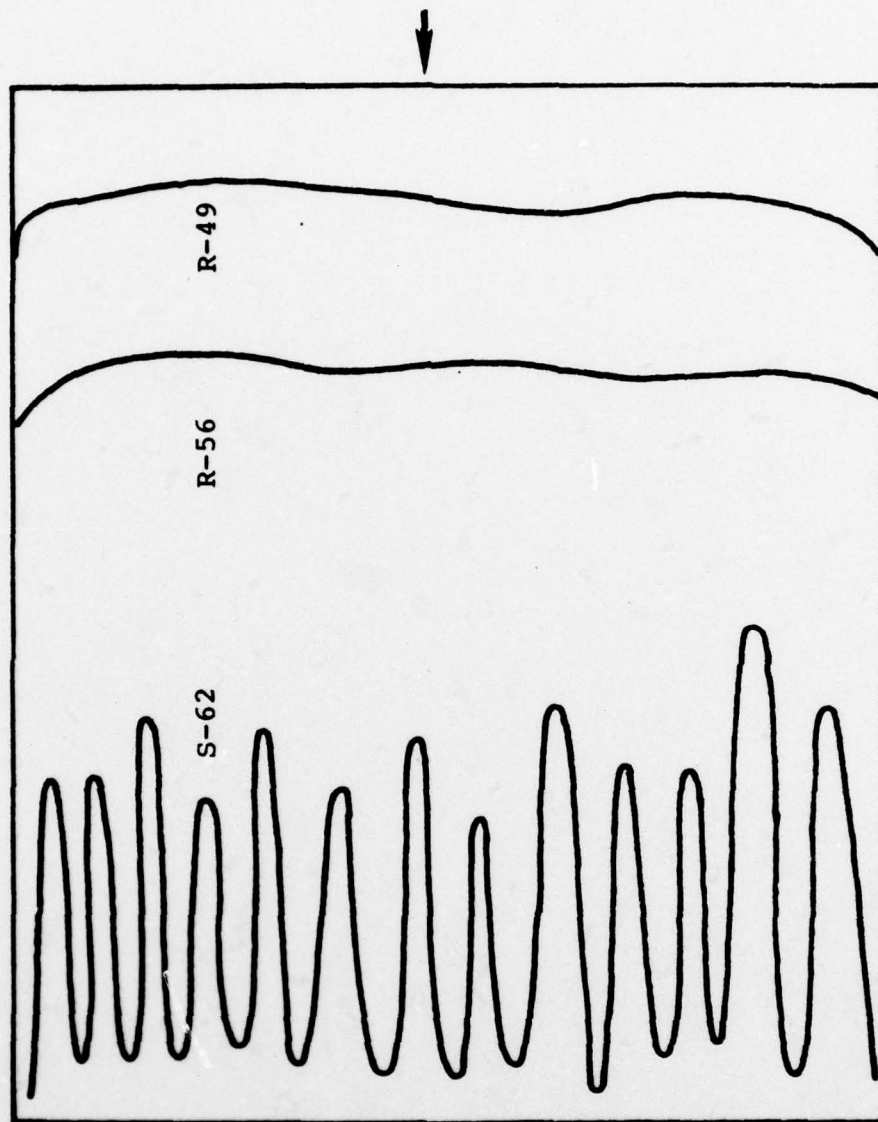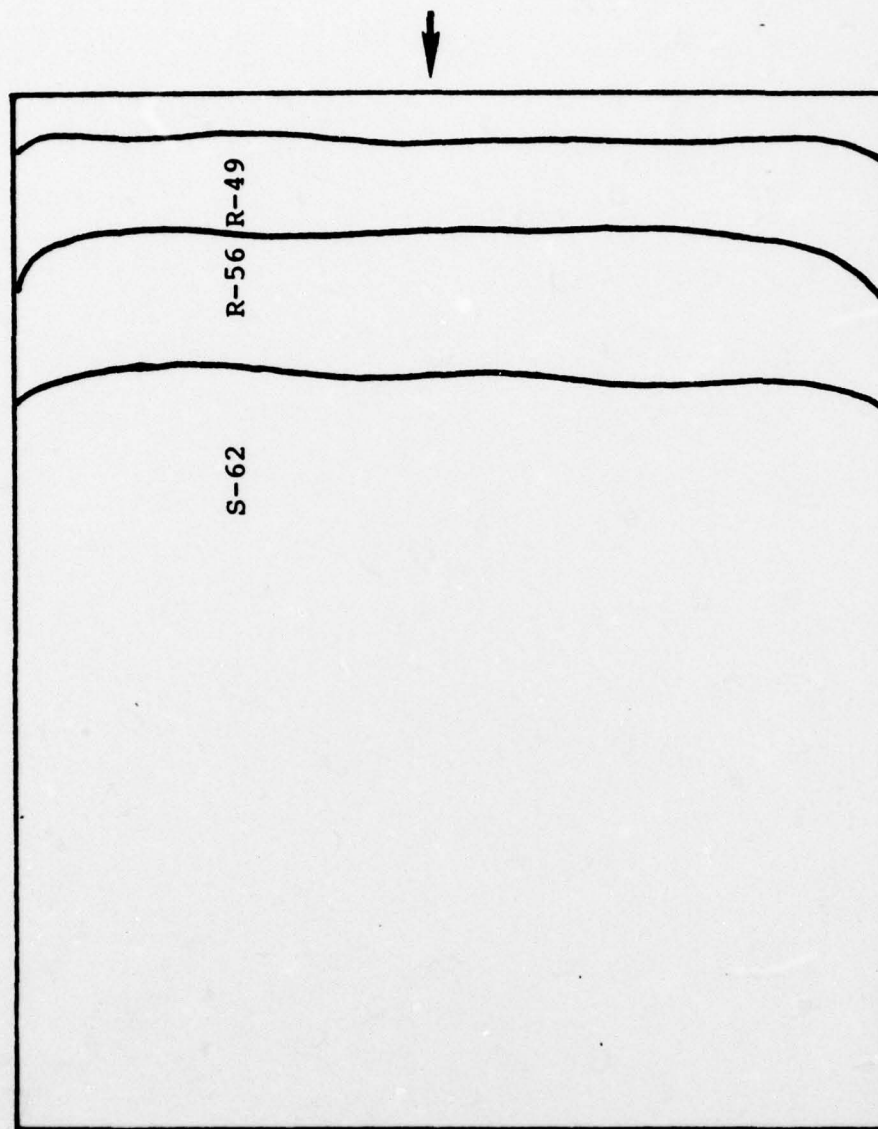Figure 13. Distribution of Liquid Crystal Color Bands in Curved Test Section for Re = 386 (De = 56)

Figure 14. Distribution of Liquid Crystal Color Bands in Curved Test Section for Re = 258 (De = 38)

R-49

R-56

S-62

The plot of the natural logarithm of the Dean number versus the natural logarithm of the Nusselt number for the curved section was then analyzed, and straight lines were fitted through the results in each region using least squares regression. These are shown in Figure 10. The slopes of these lines for the regions of highest and lowest values of Dean number were determined as respectively 0.557 and 0.591 while in the transition region the slope was 1.57. The limiting values of Dean number for the transition region were calculated from the plot as 57.1 and 67.4. Three correlations expressing the Nusselt number as a function of the Dean number for each one of the regions were determined as follows:

1. <u>Low Values of Dean Number</u> (De < 57.1)

$$\overline{Nu} = 0.292 \, De^{0.591}$$

2. <u>Transition Region</u> (57.1 < De < 67.4)

$$\overline{Nu} = 0.00556 \, De^{1.57}$$

3. <u>High Values of Dean Number</u> (De > 67.4)

$$\overline{Nu} = 0.395 \, De^{0.557}$$

54

A single correlation for the overall range of Dean numbers was also determined as:

$$\overline{Nu} = 0.171 \ De^{0.739}$$

V. DISCUSSION AND CONCLUSIONS

The measurement of the surface temperature of the unheated plate in the straight test section showed that this temperature was very close to the bulk temperature of the fluid.

It was then assumed that in the absence of significant difference in temperature between the inner wall and the air flow, the heat convected to the air was exclusively from the heated wall. Based on this assumption it was decided to compare the results of the present study for the straight test section with the analytical solution of the same problem developed by McCuen, et al. [Ref. 18]. The hydraulic diameter of the channel was calculated as Dh = 1.239 cm, and the values of Reynolds number based on the hydraulic diameter as used by McCuen also were determined. A dimensionless axial length coordinate $\bar{x}$, given by

$$\bar{x} = \frac{x}{Dh\ Re\ Pr}$$

where Pr was the Prandtl number, was calculated for x = 29.2 cm (length of the straight test section) for all the experiments. Based on the values of $\bar{x}$ it was determined that the development of the experiments would occur essentially in the thermal entrance region, and it was decided to integrate the expression of the local Nusselt number

56

for small values of $\bar{x}$

$$Nu = \frac{1}{0.67095 \, \bar{x}^{-1/3} - 2(1 + \frac{Qwi}{Qwo}) \, \bar{x}}$$

given by McCuen, et al., in order to obtain the following
expression for the average Nusselt number.

$$\overline{Nu} = - \frac{3}{4(1 + \frac{Qwi}{Qwo}) \bar{x}} \ln[1 - \frac{2}{0.67095}(1 + \frac{Qwi}{Qwo}) \bar{x}^{2/3}]$$

In this expression Qwi was the heat convected to the air
from the unheated wall, and Qwo was the heat convected
from the outer Temsheet wall. The average Nusselt numbers
were then calculated with the expression developed above
where, in accordance with the previous assumption, the
value of Qwi was taken as zero and the value of Qwo was
considered to be the same as Qair.

The average Nusselt numbers obtained from the experi-
mental data in the straight section were recalculated as
function of the hydraulic diameter and were plotted versus
Reynolds number as shown in Figure 15 along with the
analytical expression from McCuen. The only significant
difference observed for the lowest value of Reynolds
number may be explained by the fact that the value of $\bar{x}$
was equal to 0.064. In this case the Nusselt number
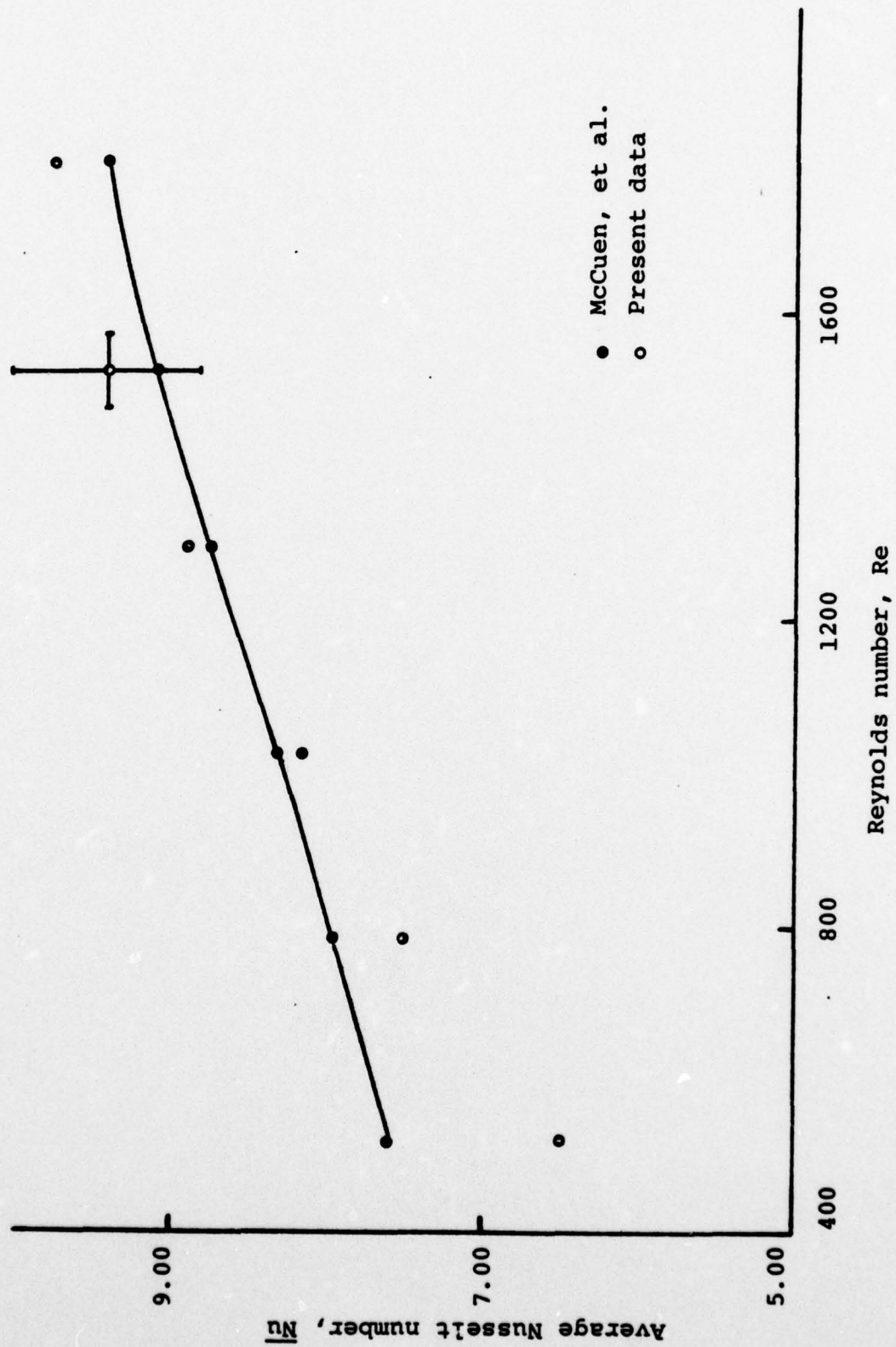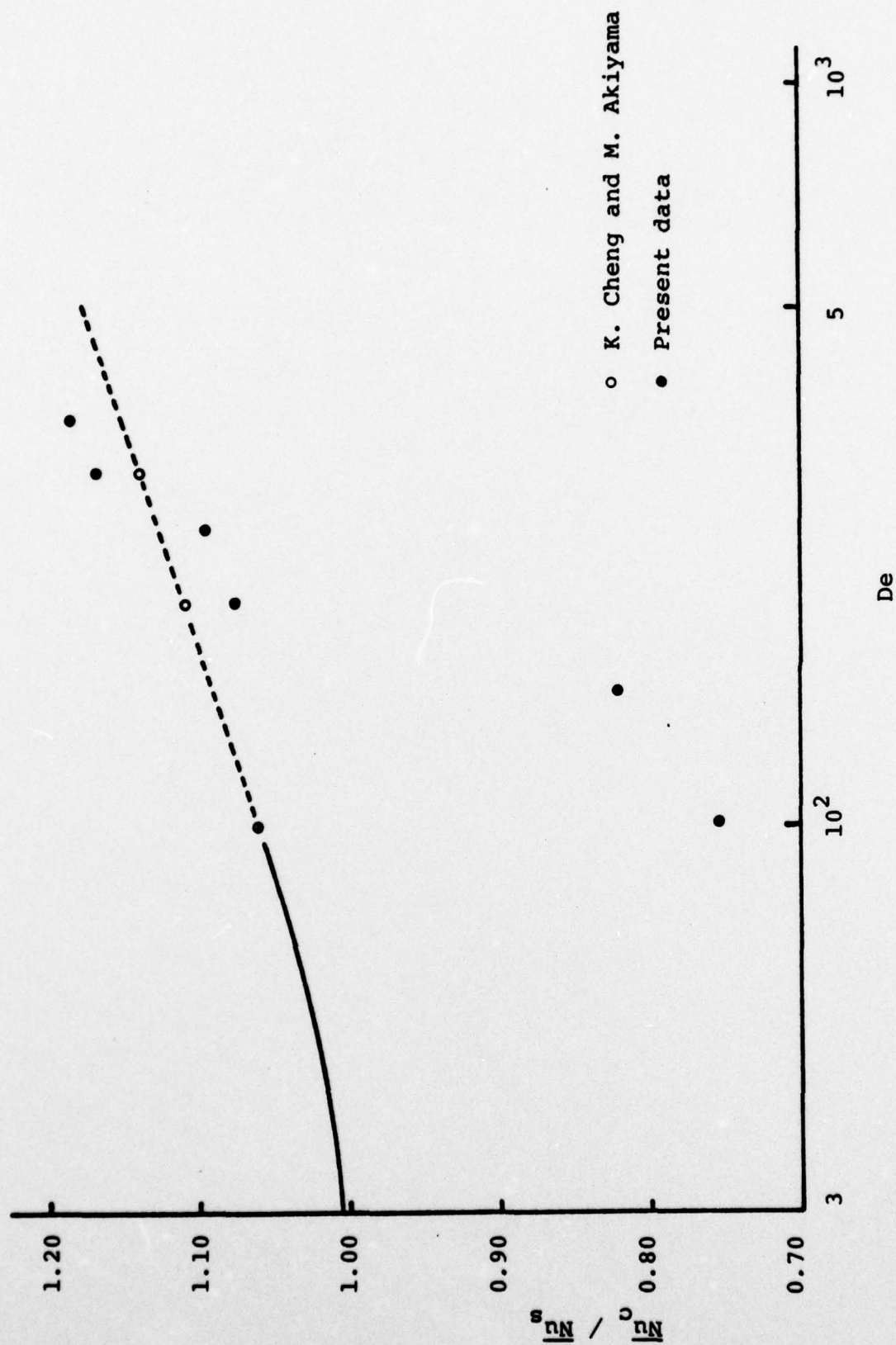expression for small values of $\bar{x}$ is probably not valid.

57

Figure 15. Comparison of Present Data with the Study by McCuen, et al.

A comparison of the data from the curved section with the analytical study by Cheng and Akiyama [Ref. 15] was attempted also for the curved test section, but the results were less conclusive. Their investigation was done for small aspect ratios (nearly square cross section), and the results were plotted only for small values of Dean number. An extrapolation of these results to greater values of Dean number for the case of the largest aspect ratio (5 to 1) is shown in Figure 16 simultaneously with the results of the present study.

After these comparisons, several conclusions about the heat transfer in rectangular channels were developed from the results obtained in the present investigation. The heat transfer rates were demonstrated to increase with increasing values of Reynolds number in both test sections. The values of the average Nusselt number for the curved section when compared with the values for the straight section seemed to indicate that there are three distinct regions of Reynolds or Dean number which can be considered. These regions were: an initial region for the lowest values of Dean number where the heat transfer rates from the straight test section were greater than from the curved test section, a final region for the highest values of Dean number where the opposite was true and a transition region for the intermediate values of Dean number.

Figure 16. Comparison of Present Data with the Study by K. Cheng and M. Akiyama

The observation of the presence of Taylor-Goertler vortices at values of Dean number for which the heat transfer rates were greater from the curved test section led to the conclusion that the overall effect of the vortices was to improve the heat transfer process from the curved section whenever their presence occurred. The critical value of Dean number for the onset of the vortices was determined from Figure 10 as 57.1.

Finally it seemed apparent from the comparison with the work of Cheng and Akiyama that for values of aspect ratio greater than five the results are independent of the aspect ratio.

VI.   RECOMMENDATIONS

Several recommendations can be made to improve the experimental study of heat transfer in curved as well as straight rectangular channels. More experiments should be performed in the transition region of the Dean number for the curved test section. This would permit a better understanding of the variation of the average Nusselt number with the Dean number and a more rigorous estimate of the critical value of Dean number above which the Taylor-Goertler vortices will form. The effect of the vortices on the heat transfer from the curved section could then be explained with more detail, and improved correlations for the average Nusselt number as a function of the Dean number could be developed.

With respect to the apparatus, it became apparent that an improved method of suspending the thermocouples in the flow to measure T_{IN} and T_{OUT} should be devised. Considerable thought must be given to this problem in order to eliminate the interaction between the Plexiglas and the beads of the thermocouples and also to make the distance between the beads and the plates more uniform for all the suspended thermocouples. The surface temperature of the inner wall should be measured in future experiments.

Finally, a motion picture study of the onset of the Taylor-Goertler vortices in the curved test section, using the liquid crystals, would be possible and of great interest.

APPENDIX A

ERROR ANALYSIS

The uncertainties for the major variables in the experiments were calculated in accordance with the method described by S. Kline and F. McClintoch [Ref. 22]. The estimates of the uncertainty in the measured quantities were made quite conservatively so that there was considerable confidence in the calculated uncertainties. As an example, the calculation of the uncertainty in the Reynolds number is given below. The Reynolds number was defined by the equation:

$$Re = \frac{\rho U d}{\mu}$$

and the uncertainty was calculated as:

$$\frac{dRe}{Re} = \sqrt{\left(\frac{d\rho}{\rho}\right)^2 + \left(\frac{dU}{U}\right)^2 + \left(\frac{dd}{d}\right)^2 + \left(\frac{d\mu}{\mu}\right)^2}$$

The uncertainty in the flow velocity was determined as $\frac{dU}{U} = 0.02176$ from similar calculations based on estimates of the uncertainties in the cross sectional area of the channel and in the reading of the volumetric flow rate. The uncertainties in the density, the height of the channel and the dynamic viscosity were obtained from estimates as

63

$\frac{d\rho}{\rho} = 0.00082$, $\frac{dd}{d} = 0.02000$ and $\frac{d\mu}{\mu}$ as 0.00223. The uncertainty in the Reynolds number was then calculated as

$$\frac{dRe}{Re} = \sqrt{(0.00082)^2 + (0.02176)^2 + (0.02)^2 + (0.00223)^2} = 0.02965$$

The uncertainty in the Nusselt number was computed with the expression:

$$\frac{dNu}{Nu} = \sqrt{(\frac{dK}{K})^2 + (\frac{d\rho}{\rho})^2 + (\frac{dC_p}{C_p})^2 + (\frac{d\dot{q}}{\dot{q}})^2 + (\frac{d\Delta T}{\Delta T})^2 + (\frac{dA_{PL}}{A_{PL}})^2 + (\frac{dd}{d})^2 + (\frac{dT_{OUT} - T_{IN}}{T_{OUT} - T_{IN}})^2}$$

The values of the uncertainties for other variables are listed below.

Quantity	Uncertainty
Ac	0.02010
A_{PL}	0.00265
Cp	0.00415
De	0.03576
$\overline{h}$	0.06242
Kair	0.00038
$\overline{Nu}$	0.06555
$\dot{q}$	0.00835
Qair	0.04050
Re	0.02965

Quantity	Uncertainty
T_B	0.01640
T_{IN}	0.00453
T_{OUT}	0.01060
T_W	0.03207
$T_{OUT} - T_{IN}$	0.03940
$\Delta T = T_W - T_B$	0.04743
μ	0.00223
ρ	0.00082

APPENDIX B

SAMPLE CALCULATIONS

A sketch of the control volume for the energy balance
on the straight test section indicating the major heat
transfer components involved is shown in Figure 17. A
similar diagram could be considered for the curved test
section. Sample calculations of the power supplied (Qp),
the heat convected to the air ($Qair$), the heat lost through
the insulation (Q_{LO}), the radiated heat transfer (Q_R),
the average heat transfer coefficient ($\bar{h}$), the average
Nusselt number ($\overline{Nu}$) and the Reynolds number (Re) are given
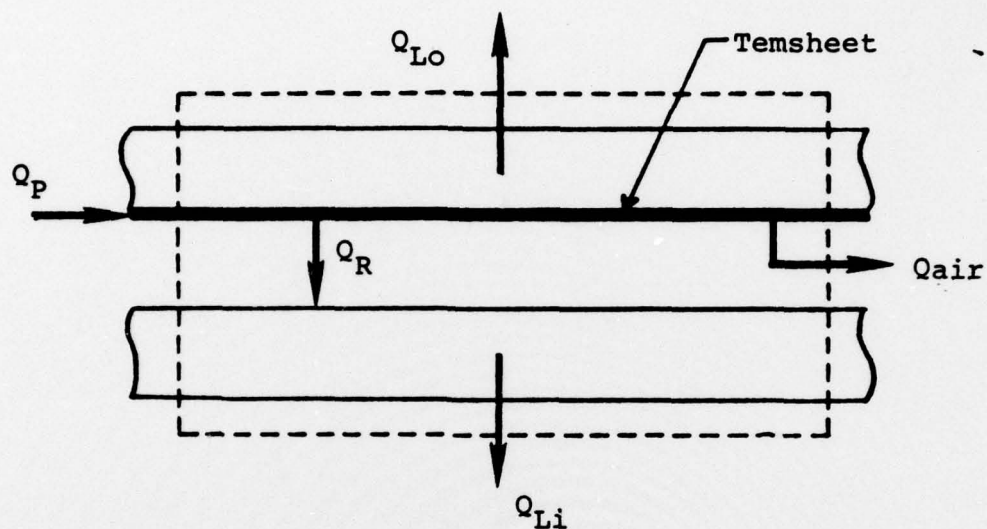below for the straight test section.

ENERGY BALANCE

Figure 17.   Energy Balance in Straight Test Section

SAMPLE CALCULATIONS

A.   DATA

T_{ROOM} = 23.8 °C

$\dot{q}$ = 0.126 m^3/min

V_{PR} = 3.223 V

V_H = 35.580 V

R_{PR} = 2.013 Ω

T_{INS1} = 1.997 mv = 49.13 °C

T_{INS2} = 1.542 mv = 38.33 °C

T_{IN1} = 0.963 mv = 24.29 °C

T_{IN2} = 0.962 mv = 24.27 °C

67

T_{IN3} = 0.955 mv = 24.10 °C

T_{IN4} = 0.965 mv = 24.34 °C

T_{EXIT} = 1.072 mv = 26.97 °C

Two1 = 2.684 mv = 64.93 °C

Two2 = 2.432 mv = 59.19 °C

T_{OUT1} = 1.591 mv = 39.52 °C

T_{OUT2} = 1.606 mv = 39.87 °C

T_{OUT3} = 1.527 mv = 37.97 °C

T_{OUT4} = 1.662 mv = 41.21 °C

Twi1 = 1.417 mv = 35.34 °C

Twi2 = 1.265 mv = 31.66 °C

A_{PL} = 0.0742 m^2

A_c = 0.0016 m^2

d = 0.00635 m

Kair = 0.02662 W/m °C

Cpair = 1.0057 KJ/Kg °C (0.241 BTU/lbm °F)

μair = 1.983 x 10^{-5} Kg/m·sec

K_{INS} = 4.18 x 10^{-2} W/m °C

ΔX_{INS} = 0.00635 m

ε_{wo} = 0.90

ε_{wi} = 0.75

Fwo-wi = 1.0

σ = 5.669 x 10^{-8} W/m^2 °K

B. TEMPERATURE CALCULATIONS

1. <u>Average Inlet Temperature</u> (T_{IN})

$$T_{IN} = \frac{T_{IN1} + T_{IN2} + T_{IN3} + T_{IN4}}{4}$$

$$= \frac{24.29 + 24.27 + 24.10 + 24.34}{4}$$

$$= 24.25 \ °C$$

2. <u>Average Outlet Temperature</u> (T_{OUT})

$$T_{OUT} = \frac{T_{OUT1} + T_{OUT2} + T_{OUT3} + T_{OUT4}}{4}$$

$$= \frac{39.52 + 39.87 + 37.97 + 41.21}{4}$$

$$= 39.64 \ °C$$

3. <u>Temperature Difference in Insulation</u> (ΔT_{INS})

$$\Delta T_{INS} = T_{INS1} - T_{INS2} = 49.13 - 38.33 = 10.80 \ °C$$

4. <u>Average Temperature of Outer Plate</u> (T_{wo})

$$T_{wo} = \frac{T_{wo1} + T_{wo2}}{2} = \frac{64.93 + 59.19}{2}$$

$$= 62.06 \ °C = 335.06 \ °K$$

5. **Average Temperature of Inner Plate** (T_{wi})

$$T_{wi} = \frac{T_{wi1} + T_{wi2}}{2} = \frac{35.34 + 31.66}{2}$$

$$= 33.50\ °C = 306.50\ °K$$

6. **Bulk Temperature** (T_B)

$$T_B = \frac{T_{IN} + T_{OUT}}{2} = \frac{24.25 + 39.64}{2} = 31.95\ °C$$

7. **Mean Temperature Difference** (ΔT)

$$\Delta T = T_{wo} - T_B = 62.06 - 31.95 = 30.11\ °C$$

C. **POWER CALCULATIONS**

1. **Power Supplied** (Q_p)

$$Q_p = \frac{V_{PR}\,V_H}{R_{PR}} = \frac{(35.580)(3.223)}{2.013} = 56.97\ W$$

2. **Heat Lost Through Outer Plate** (Q_{LO})

$$Q_{LO} = \frac{\Delta T_{INS}}{\Delta X_{INS}/K_{INS}\,A_{PL}}$$

$$= \frac{10.80}{(0.00635)/(4.18 \times 10^{-2})(0.0742))} = 5.27\ W$$

3. <u>Heat Radiated</u> (Q_R)

    a. <u>Radiation Resistance</u> (R_R)

$$R_R = \frac{1 - \varepsilon_{wo}}{A_{PL} \varepsilon_{wo}} + \frac{1}{A_{PL} F_{wo-wi}} + \frac{1 - \varepsilon_{wi}}{A_{PL} \varepsilon_{wi}}$$

$$= \frac{1}{A_{PL}} \left[\frac{1}{\varepsilon_{wo}} + \frac{1}{\varepsilon_{wi}} - 1\right] = \frac{1.444}{A_{PL}}$$

    b. <u>Heat Radiated</u> (Q_R)

$$Q_R = \frac{\sigma (T_{wo}^4 - T_{wi}^4)}{R_R}$$

$$= \frac{(5.669 \times 10^{-8})(0.0742)(335.1^4 - 306.5^4)}{(1.444)}$$

$$= 11.02 \text{ W}$$

4. <u>Heat Convected to the Air</u> (Qair)

    a. <u>Volumetric Flow Rate</u>

$$\dot{q} = \frac{(0.314)(0.4)}{60} = 0.00209 \text{ m}^3/\text{sec}$$

    b. <u>Density</u>

$$\rho = \frac{p}{RT} = \frac{1.0132 \times 10^5}{(287)(26.97 + 273)}$$

$$= 1.177 \text{ Kg/m}^3 \ (0.073 \text{ lbm/ft}^3)$$

c. <u>Heat Convected</u> (Q_{air})

$$Q_{air} = \rho\, \dot{q}\, C_P\, (T_{OUT} - T_{IN})$$

$$= (1.177)(0.00209)(1.0057)(39.64 - 24.25)$$

$$= 0.03825\ \text{KJ/sec}$$

$$= 38.25\ \text{W}$$

D. AVERAGE HEAT TRANSFER COEFFICIENT

$$\bar{h} = \frac{Q_{air}}{A_{PL}\,\Delta T} = \frac{38.25}{(0.0742)(30.11)}$$

$$= 17.12\ \text{W/m}^2\ {}^\circ\text{C}$$

E. AVERAGE NUSSELT NUMBER

$$\overline{Nu} = \frac{\bar{h}\, d}{K_{air}} = \frac{(17.12)(0.00635)}{(0.02662)} = 4.084$$

F. REYNOLDS NUMBER

1. <u>Mean Velocity</u> (U)

$$U = \frac{\dot{q}}{A_c} = \frac{0.00209}{0.0016} = 1.30625\ \text{m/sec}$$

2. <u>Reynolds Number</u> (Re)

$$Re \ = \ \frac{\rho \ U \ d}{\mu} \ = \ \frac{(1.177)(1.30625)(0.00635)}{(1.983 \times 10^{-5})}$$

$$= \ 492.33$$

$$Re \ = \ 492$$

LIST OF REFERENCES

1. Lord Rayleigh, "On the Dynamics of Revolving Fluids,"
    Proceedings of the Royal Society of London, series A
    v. 93, pp. 148-154, 1916. Reprints in Scientific
    Papers v. 6, pp. 447-453.

2. Taylor, G.I., "Stability of a Viscous Liquid Contained
    Between Two Rotating Cylinders," Philosophical Trans-
    actions of the Royal Society of London, Series A,
    v. 223, pp. 289-343, 1923.

3. Dean, W.R., "Fluid Motion in a Curved Channel,"
    Proceedings of the Royal Society of London, series A,
    v. 121, pp. 402-420, 1928.

4. Reid, W.H., "On the Stability of Viscous Flow in a
    Curved Channel," Proceedings of the Royal Society of
    London, series A, v. 244, pp. 186-198, 1958.

5. National Advisory Committee for Aeronautics, Technical
    Memorandum 1375, On the Three Dimensional Instability
    of Laminar Boundary Layers on Concave Walls, by
    H. Goertler, 1942.

6. Schlichting, H., Boundary Layer Theory, 6th ed.,
    pp. 500-522, McGraw-Hill, 1968.

7. Smith, A.M.O., "On the Growth of Taylor-Goertler
    Vortices Along Highly Concave Walls," Quarterly of
    Applied Mathematics, v. 8, pp. 233-262, November 1955.

8. Kreith, F., "The Influence of Curvature on Heat Transfer
    to Incompressible Fluids," Trans. ASME, v. 77, pp. 1247-
    1256, 1955.

9. Aerospace Research Laboratories Report ARL 65-68,
    A Simplified Approach to the Influence of Goertler
    Type Vortices on the Heat-Transfer from a Wall, by
    Lief N. Persen, May 1965.

10. McCormack, P.D., Welker, H., and Kelleher, M.,
    "Taylor-Goertler Vortices and Their Effect on Heat
    Transfer," Journal of Heat Transfer, v. 92, pp. 101-
    112, February 1970.

11. Kahawita, R. and Meroney, R., "The Influence of Heating
    on the Stability of Laminar Boundary Layers Along Concave
    Curved Walls," Journal of Applied Mechanics, v. 99,
    pp. 11-17, March 1977.

12. Mori, Y. and Uchida, Y., "Forced Convective Heat
    Transfer Between Horizontal Flat Plates," International
    Journal of Heat and Mass Transfer, v. 9, pp. 803-817,
    1966.

13. Akiyama, M., Hwang, G.J., and Cheng, K.C., "Experiments
    on the Onset of Longitudinal Vortices in Laminar
    Forced Convection Between Horizontal Plates," Journal
    of Heat Transfer, v. 93, pp. 335-341, November 1971.

14. Department of Mechanical Engineering, Stanford University,
    Technical Report No. 75, Laminar Flow Forced Convection
    Heat Transfer and Flow Friction in Straight and Curved
    Ducts - A Summary of Analytical Solutions, by R.K. Shah
    and A.L. London, November 1971.

15. Cheng, K.C. and Akiyama, M., "Laminar Forced Convection
    Heat Transfer in Curved Rectangular Channels," International
    Journal of Heat and Mass Transfer, v. 13, pp. 471-490,
    1970.

16. Mori, Y., Uchida, Y., and Ukon, T., "Forced Convective
    Heat Transfer in a Curved Channel with a Square Cross
    Section," International Journal of Heat and Mass Transfer,
    v. 14, pp. 1787-1805, 1971.

17. Cheng, K.C., Lin, R.C., and Ou, J.W., Graetz Problem in
    Curved Square Channels, ASME paper No. 75-HT-EE,
    San Francisco, California, 11 August 1975.

18. Department of Mechanical Engineering, Stanford University,
    Report No. AHT-3, Heat Transfer with Laminar and
    Turbulent Flow Between Parallel Planes with Constant
    and Variable Wall Temperature and Heat Flux, by P.A.
    McCuen, W.M. Kays, and W.C. Reynolds, 12 April 1962.

19. McKee, R.J., An Experimental Study of Taylor-Goertler
    Vortices in a Curved Rectangular Channel, Eng. Thesis,
    Naval Postgraduate School, Monterey, June 1973.

20. Flentie, D.L., An Experimental Study of Taylor-Goertler
    Vortices in a Curved Rectangular Channel, M.S. Thesis,
    Naval Postgraduate School, Monterey, March 1975.

21. Cooper, T.E., Field, R.J., and Meyer, J.F., "Liquid
    Crystal Thermography and Its Application to the Study
    of Convective Heat Transfer," Journal of Heat Transfer,
    v. 97, pp. 442-450, August 1975.

22. Kline, S.J. and McClintock, F.A., "Describing Uncertainties in Single-Sample Experiments," Mechanical Engineering, v. 75, pp. 3-8, January 1953.

23. Holman, J.P., Experimental Methods for Engineers, pp. 36-40, McGraw-Hill, 1966.

24. Holman, J.P., Heat Transfer, 3rd ed., pp. 125-298, McGraw-Hill, 1972.

25. Kays, W.M., Convective Heat and Mass Transfer, pp. 116-133, McGraw-Hill, 1966.

26. Knudsen, J.G. and Katz, D.L., Fluid Dynamics and Heat Transfer, pp. 382-388, McGraw-Hill, 1958.

INITIAL DISTRIBUTION LIST

No. Copies

1. Defense Documentation Center   2
   Cameron Station
   Alexandria, Virginia 22314

2. Library, Code 0142   2
   Naval Postgraduate School
   Monterey, California 93940

3. Associate Professor M. Kelleher, Code 69Kk   2
   Department of Mechanical Engineering
   Naval Postgraduate School
   Monterey, California 93940

4. LT. Mario C. Durão, Portuguese Navy   4
   LOTE No. 119
   BELVERDE - AMORA
   PORTUGAL

5. Department of Mechanical Engineering   1
   Naval Postgraduate School
   Monterey, California 93940